Science of the Total Environment 767 (2021) 145305

Contents lists available at ScienceDirect

Science of the Total Environment

journal homepage: www.elsevier.com/locate/scitotenv

Review

Formation and mechanisms of nano-metal oxide-biochar composites for pollutants removal: A review

Chenxi Zhao [a,b], Bing Wang [c,d,e,*], Benny K.G. Theng [f], Pan Wu [c,d,e], Fang Liu [c,d,e], Shengsen Wang [g], Xinqing Lee [a], Miao Chen [c,d,e], Ling Li [a], Xueyang Zhang [h]

[a] State Key Laboratory of Environmental Geochemistry, Institute of Geochemistry, Chinese Academy of Sciences, Guiyang 550081, China
[b] University of Chinese Academy of Sciences, Beijing 100049, China
[c] College of Resource and Environmental Engineering, Guizhou University, Guiyang 550025, Guizhou, China
[d] Key Laboratory of Karst Georesources and Environment, Ministry of Education, Guizhou University, Guiyang 550025, China
[e] Guizhou Karst Environmental Ecosystems Observation and Research Station, Ministry of Education, Guiyang 550025, China
[f] Manaaki Whenua-Landcare Research, Palmerston North 4442, New Zealand
[g] College of Environmental Science and Engineering, Yangzhou University, Yangzhou 225127, China
[h] School of Environmental Engineering, Jiangsu Key Laboratory of Industrial Pollution Control and Resource Reuse, Xuzhou University of Technology, Xuzhou 221018, China

HIGHLIGHTS

- Typical preparation methods for NMOBCs were summarized.
- The influencing factors on the adsorption capacity of NMOBCs are analyzed.
- The adsorption performance for different pollutants are summarized.
- Possible removal mechanisms of different pollutants were discussed.
- Suggestions and perspectives for future studies are proposed.

GRAPHICAL ABSTRACT

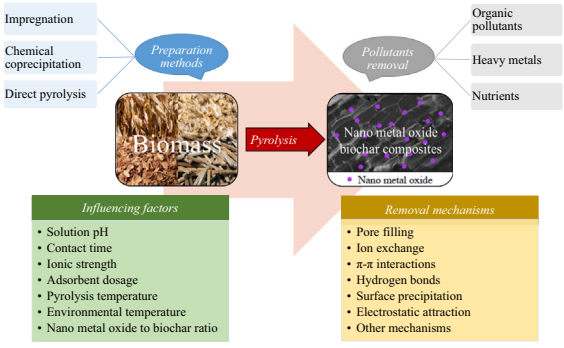

ARTICLE INFO

Article history:
Received 2 November 2020
Received in revised form 11 January 2021
Accepted 16 January 2021
Available online 22 January 2021

Editor: Deyi Hou

Keywords:
Biochar
Nano-metal oxides
Pollution remediation
Adsorption

ABSTRACT

Biochar, a carbon-rich material, has been widely used to adsorb a range of pollutants because of its low cost, large specific surface area (SSA), and high ion exchange capacity. The adsorption capacity of biochar, however, is limited by its small porosity and low content of surface functional groups. Nano-metal oxides have a large SSA and high surface energy but tend to aggregate and passivate because of their fine-grained nature. In combining the positive qualities of both biochar and nano-metal oxides, nano-metal oxide-biochar composites (NMOBCs) have emerged as a group of effective and novel adsorbents. NMOBCs improve the dispersity and stability of nano-metal oxides, rich in adsorption sites and surface functional groups, maximize the adsorption capacity of biochar and nano-metal oxides respectively. Since the adsorption capacity and mechanisms of NMOBCs vary greatly amongst different preparations and application conditions, there is a need for a review of NMOBCs. Herein we firstly summarize the recent methods of preparing NMOBCs, the factors influencing their efficacy in the removal of several pollutants, mechanisms underlying the adsorption of different pollutants, and their potential applications for pollution control. Recommendations and suggestions for future studies on NMOBCs are also proposed.

* Corresponding author at: College of Resource and Environmental Engineering, Guizhou University, Guiyang 550025, Guizhou, China.
E-mail address: bwang6@gzu.edu.cn (B. Wang).

https://doi.org/10.1016/j.scitotenv.2021.145305
0048-9697/

Contents

1. Introduction

Biochar is a carbon-rich material that was first discovered in the Amazon basin (Kim et al., 2007; Lehmann and Joseph, 2009). It is commonly produced by pyrolysis of agricultural and forestry wastes, manure, and organic solid wastes under limited oxygen supply and at moderate temperatures (<700 °C) (Lehmann and Joseph, 2009; O'Connor et al., 2018; Wang et al., 2020c). Furthermore, biochar can also be obtained by other means, such as gasification and hydrothermal carbonization (Cha et al., 2016; Ok et al., 2020). Following early studies on the roles of biochar in carbon sequestration, attention has been directed at using biochar to control seedling growth, soil water release, and as a soil amendment (Lehmann and Joseph, 2009; Mandal et al., 2020a; Wang et al., 2020b; Wen et al., 2020). Interestingly, biochar has been used as an effective adsorbent of environmental pollutants (Qian et al., 2015).

Pristine biochar has unique surface chemical properties such as high specific surface area (SSA), alkalinity, aromaticity, and multiple surface functional groups (Mandal et al., 2020b; Shi et al., 2019). It shows variable affinities and propensities for adsorbing pollutants (Ahmad et al., 2014; Yao et al., 2013a), pristine biochar has a relatively limited adsorption capacity of pollutants (Zhang et al., 2020a). A great deal of researches have therefore been directed at modifying biochar by biological, physical, and chemical means (Wang et al., 2017; Wang et al., 2015a; Zhao et al., 2020). The chemical modification involves treatment with acid, alkali, oxidizing agents, and metal salts (Wang and Wang, 2019; Wang et al., 2018d). Acid-treated biochar has a larger SSA and oxygen-containing functional groups than its pristine counterpart (Ahmed et al., 2016). Similar changes occur in the physicochemical properties of biochar that have been chemically modified by alkali, oxidant, and a metal salt. These modifications, however, are challenging to make routinely. They may also decrease pore volume (Ahmed et al., 2016), and cause secondary pollution (Wang et al., 2018c).

Nano-metal oxides are a group of metal oxide materials with sizes ranging from 1 to 100 nm. Due to their nanometer size, they have relatively high SSA, active surface, diffusion activation energy, and strong quantum effect (Wang et al., 2019d). Nano-metal oxides generally have improved redox and adsorption capability, are inexpensive and environmentally friendly. In recent years, nano-metal oxides have been produced and used for environmental remediation (Penke et al., 2019; Yuan et al., 2020). Biochar modified with nano-metal oxides has a larger SSA, cation exchange capacity, and porosity than the pristine material as well as being enriched in surface functional groups. The capacity of modified biochar for adsorbing pollutants varies with the type of nano-metal oxides (Dewage et al., 2018; Hu et al., 2019; Oginni et al., 2020). Because of their large SSA and high reactivity (Bhateria and Singh, 2019), nano-metal oxides can effectively remove environmental pollutants, especially heavy metals, from aqueous solutions (Dasgupta et al., 2017). The following nano-metal oxides have been used to modify biochar: (1) unary oxides such as MgO, ZnO, Fe_2O_3, MnO_2 (Song et al., 2014; Wang et al., 2019e; Xu et al., 2020a; Zhang et al., 2012; Zhu et al., 2018); (2) binary oxides such as $MnFe_2O_4$, $MnAl_2O_4$ (Lai et al., 2019; Peng et al., 2020; Yin et al., 2020); and (3) ternary oxides such as $CuZnFe_2O_4$, HA/Fe-Mn oxides (Guo et al., 2019; Heo et al., 2019).

Combining the advantages of biochar and nano-metal oxides respectively, novel nano-metal oxide-biochar composites (NMOBCs) are more dispersible, have a smaller crystallite size, and a higher electron transfer capacity than unmodified biochar (Wang et al., 2019d). Unlike nano-metal oxides, NMOBCs do not readily agglomerate and passivate (Liu et al., 2020; Wang et al., 2019c). Besides, they are rich in adsorption sites and surface functional groups. As such, NMOBCs can adsorb a variety of organic pollutants, including antibiotics, organic dyes, and bisphenol A (BPA) (Li et al., 2018b; Luo et al., 2019; Zheng et al., 2020), heavy metals, such as Cd, Cr, Cu, As, Pb (Saravanakumar et al., 2019; Wan et al., 2020; Yu et al., 2018; Yu et al., 2017; Zhang et al., 2020b; Zhou et al., 2018), phosphates (Tang et al., 2019), and nitrates (Li et al., 2020b; Li et al., 2017). However, the physicochemical properties, adsorption performance and mechanisms for various pollutants of NMOBCs have rarely been systematically summarized. Since NMOBCs are obtained under different conditions and using different feedstocks, the performance for adsorbing pollutants is variable. Differences in physicochemical properties among NMOBCs also lead to variation in adsorption mechanisms and data interpretations. For instance, the adsorption capacity of nano-MnO_2-biochar composite for Pb(II) reached 305.25 mg/g (Tan et al., 2018), while the adsorption capacity of that by nano-NiO-biochar composite was only 28.0 mg/g (Saravanakumar et al., 2019). The mechanisms of removing As(III) by nano-MnO_2-biochar composite were mainly ligand exchange and redox (Yu et al.,

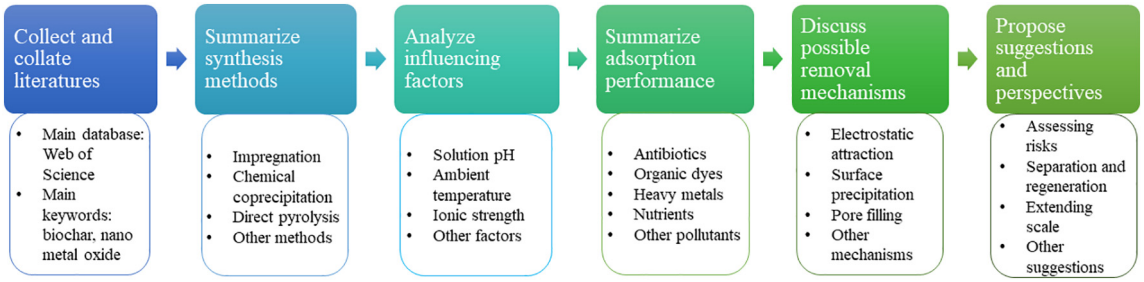

Fig. 1. Flowchart of NMOBCs' research methodology.

2015), but the mechanisms of removing As(III) by nano Fe-Mn oxide-biochar composite were attributed to surface adsorption and redox (Lin et al., 2019). Therefore, a review on the influencing factors, mechanisms, and potential applications of NMOBCs is highly needed. Herein, we assess the current information on the formation and mechanisms of NMOBCs as adsorbents for environmental pollutants and provide suggestions for further research into the potential applications of different NMOBCs. The objectives of this review are to (1) summarize typical preparation methods for NMOBCs; (2) analyze the influencing factors on adsorption capacity and mechanisms of NMOBCs; (3) discuss the possible removal mechanisms of different pollutants by NMOBCs; (4) propose suggestions and perspectives for future studies. The methodology flowchart of the research is shown in Fig. 1.

2. Synthesis of NMOBCs

Fig. 2 shows the various methods of preparing NMOBCs including impregnation, chemical coprecipitation, direct pyrolysis, and other emerging methods.

2.1. Impregnation

Impregnation is the most common method of synthesizing NMOBCs. It involves immersing the solid biochar powder in a solution containing active ingredients, allowing the latter to adhere to the solid (Zhang et al., 2020d). The resultant NMOBCs have large SSA, cation exchange capacity, and porosity as well as a high content of surface functional groups (Wang et al., 2017). Solutions of $KMnO_4$ (Lin et al., 2019; Yu et al., 2015), $MgCl_2$ (Xiao et al., 2018), and $FeSO_4{\cdot}7H_2O$ (Lin et al., 2019) are commonly used to impregnate biochar. For instance, Wang et al. (2015b) obtained a Mn-oxide biochar composite by impregnating peeled pine biochar with a 3.65% $KMnO_4$ solution. The Mn content of the composite product influenced its capacity for adsorbing Pb(II). The removal efficiency of Pb(II) reached 98.9% at pH 5.0, which was 5 times that of pristine biochar. Xiao et al. (2018) prepared biochar from sugarcane residues and impregnated it with $MgCl_2$ solution to obtain a nano-MgO-biochar composite. It was found that Cr(VI) could be adsorbed directly by the composite through chemical interaction with MgO on the surface. Lin et al. (2019) obtained a Fe/Mn oxide-biochar composite by impregnating biochar from corn stalk with $FeSO_4{\cdot}7H_2O$ and $KMnO_4$ solution. The composite contained more oxygen-functional groups than the pristine biochar, showing a maximum adsorption capacity of 8.8 mg/g for As in the pH range of 3–7. In general, impregnation is one of the simplest methods for synthesizing NMOBCs, and the NMOBCs prepared by impregnation have a relatively large capacity for adsorbing pollutants.

2.2. Chemical coprecipitation

In chemical coprecipitation, metal salts in solution are induced to precipitate and adhere to the surface of the biochar by adjusting the solution pH, chemical reduction, and other means (Luo et al., 2019). The process is inexpensive and yields homogeneous nanoparticles of high purity and accurate stoichiometry but under strict reaction

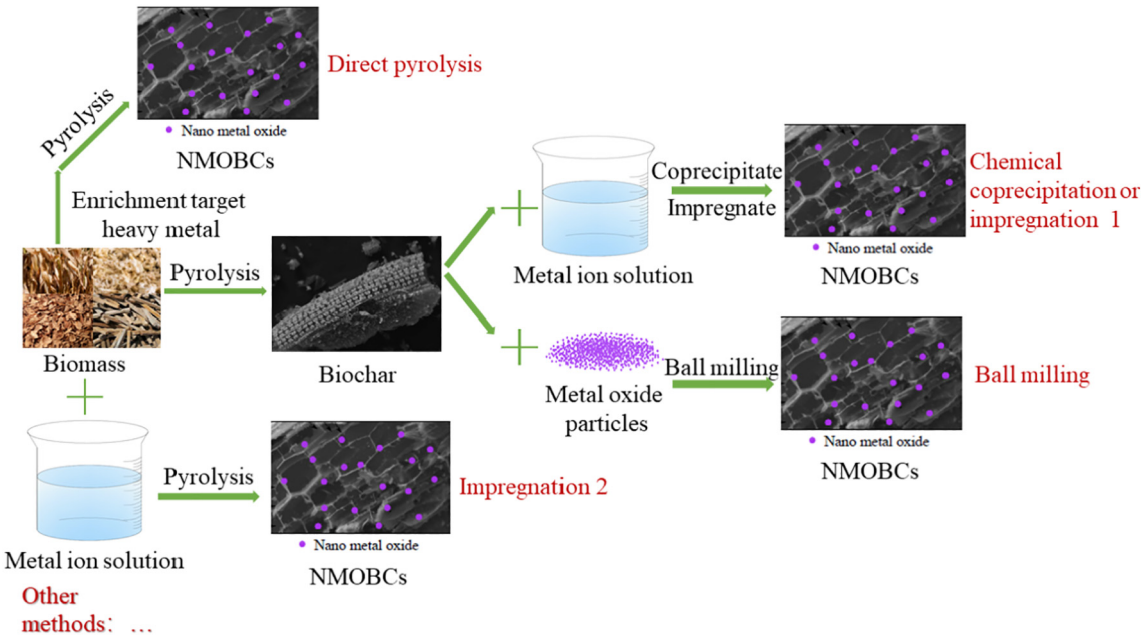

Fig. 2. Description of various synthesis methods for NMOBCs preparation.

conditions (Li et al., 2020a). It can control the relative growth rate of nucleation nanoparticles, the shape and size of the resulting product (Gharibshahian, 2020). For example, nano-MnO_2-composite was prepared by chemical coprecipitation with $MnSO_4 \cdot H_2O$ and $KMnO_4$. The self-assembled MnO_2 particles on the biochar were spherical with diameters of 200–500 nm. Compared with the pristine biochar, the adsorption capacity for oxytetracycline (OTC) increased by 0.0151 mmol/g (Gao et al., 2018). Subsequently, a magnetic NiO-biochar composite was also prepared by chemical coprecipitation with biochar derived from invasive plants and NiO from a $NiNO_3$ solution. Due to the accumulation of NiO, the SSA and pore volume of the composite are lower than those of pristine biochar. The composite, however, appeared to have a large number of active sites, capable of adsorbing Pb(II) (28.0 mg/g) (Saravanakumar et al., 2019). In addition, the nano-Cu_2O/biochar composite prepared by chemical coprecipitation of distiller grains biochar and $CuSO_4$ also showed good antibacterial performance against *Escherichia coli* (Yang et al., 2019). In general, impregnation and chemical coprecipitation are the two most common methods for preparing magnetic biochar composites (Yi et al., 2020). Compared with impregnation, chemical coprecipitation is more complicated to operate, while the physical properties of the resulting NMOBC are more controllable (Li et al., 2020a).

2.3. Direct pyrolysis

Direct pyrolysis refers to the method of preparing biochar composites by pyrolysis metal-rich biomass in an anaerobic environment (Yao et al., 2013b). Being enriched in metal oxide nanoparticles, the resultant composites are effective in pollutants removal. Li et al. (2018a) directly pyrolyzed Zn-contaminated corn stalk to produce nano-sized ZnO modified biochar. The ZnO nanoparticles were uniformly dispersed, creating an open porous structure. As a result, the composite was more effective in adsorbing pollutants than the pristine biochar. Yao et al. (2013b) directly pyrolyzed Mg-enriched tomato leaves to obtain a biochar composite containing widely distributed nanoparticles of MgO (46.0 nm in size) and $Mg(OH)_2$ (6.3 nm in size). Thus, direct pyrolysis is simpler to carry out than other preparation methods. Although this method is easy to operate, two key factors need to be fully considered when they were used, which are the selection of optimal pyrolysis temperature and availability of target biomass for pyrolysis.

2.4. Other methods

In addition to the methods mentioned above, other methods for preparing NMOBCs are also recently developed, such as ball milling and sol-gel method (Liu et al., 2019; Zheng et al., 2020).

Ball milling technology has been used to modify biochar because it is environmentally friendly and cost saving (Qin et al., 2019; Wang et al., 2018a; Wang et al., 2019a; Wang et al., 2018b). Zheng et al. (2020) used ball milling to prepare nano-MgO-biochar composite for phosphate removal. The results showed that the surface of the composite was coated with MgO nanoparticles of 20 nm diameters which were helpful for phosphate removal. Similarly, Shang et al. (2016) obtained a composite of biochar and magnetic Fe_2O_3 particles by ball milling. X-ray spectroscopy (EDS) analysis showed that the composite contained a large amount of iron oxides. This could increase its adsorption sites, which is favorable for chemisorption. In comparison with the corresponding pristine biochar, the composites prepared by ball milling have smaller particle sizes and larger SSA beneficial to the adsorption of pollutants.

The sol-gel method was used by Liu et al. (2019) to obtain a nano-size Fe_2O_3 rosin/biochar composite, in which rosin served as both a phase-transfer material and biochar-based biomass. Earlier, Khataee et al. (2017) used a modified sol-gel method to synthesize a nano-ZrO_2/biochar composite with a total pore volume of 5.951 cm^3/g and a SSA of 29.621 m^2/g. The nano-metal oxides introduced into the material were uniformly distributed in the porous bulk hydrogel, yielding a product with a uniform pore structure, and high thermal stability, mechanical strength, and adsorption performance (Wu et al., 2020b). Recently, Ali et al. (2019) prepared a nano-ZnO-biochar composite as a foliar spray to decrease the Cd accumulation in the plant and found that the accumulation of heavy metal in the plant decreased and improved plant growth.

In this respect, due to the superiority of the novel preparation methods as mentioned above, there may be more emerging and promising methods to prepare NMOBCs in the future. The advantages and disadvantages of the various methods, commonly used to prepare NMOBCs, are summarized in Table 1.

Table 1
Comparison of possible advantages and disadvantages of different methods commonly used to prepare NMOBCs.

Synthesis methods	Advantages	Disadvantages
Impregnation	Simple to operate; the composites have a large capacity for adsorbing heavy metals	May cause chemical pollution
Chemical coprecipitation	Low cost, high purity, accurate stoichiometry, homogeneous nanoparticles	Harsh reaction conditions may cause chemical pollution, more complicated than impregnation
Direct pyrolysis	Biomass already enriched with target heavy metals, facilitating the preparation process	Difficult to control the proportion of nano-metal oxides in the composites
Ball milling	Low cost, easy to operate, no chemical pollution, effective reduction of particle size of metal oxides	Easy to disperse in water, and move to surface runoff, pollutants can migrate out of the contaminated site, posing potential risks to groundwater

3. Factors influencing pollutants adsorption to NMOBCs

The adsorption of various pollutants to NMOBCs is influenced by several factors, maily including solution pH, dosage of composite, ionic strength, and ambient temperature. The following will discuss each influencing factor separately in detail (Fig. 3).

3.1. Solution pH

Solution pH has a predominant influence on the charge characteristics of NMOBCs through the protonation and deprotonation of oxygen-containing groups on the composite surface which, in turn, affects pollutants adsorption (Tan et al., 2018). When the solution pH is lower than the point of zero charge (pzc) of NMOBCs, that is $pH < pH_{pzc}$, the composite surface is positively charged, and anion adsorption is favored. On the contrary, when $pH > pH_{pzc}$, the surface charge is negative, and hence conducive to cation adsorption (Wang et al., 2020a). When the pH increases beyond a certain value (amino groups are deprotonated), the contribution of the π^+-π electron donor-acceptor interaction is suppressed, and sulfathiazole adsorption by biochar is decreased (Kim et al., 2018). Wang et al. (2015b) used a MnO_2-biochar composite (at pH_{pzc} 3.2) and obtained a maximum removal rate of Pb(II) at pH 5.0 when Pb mainly existed in the form of Pb^{2+} and $PbOH^+$, and no precipitation occurred. Chaukura et al. (2016) used a Fe_2O_3-biochar nanocomposite and observed maximum adsorption of methyl orange at pH 8.0 at which point the dye molecules existed as anions in the solution. The ZrO_2-biochar composite, prepared by Khataee et al. (2017), had a pzc of 7.35 and showed maximum adsorption of Reactive Yellow 39 at pH 6.0 when its surface was positively charged. Positively charged ZrO_2-biochar composite is also a good adsorbent of anionic dyes which, however, may be degraded by hydroxyl produced during the reaction. The adsorption of organic dyes by

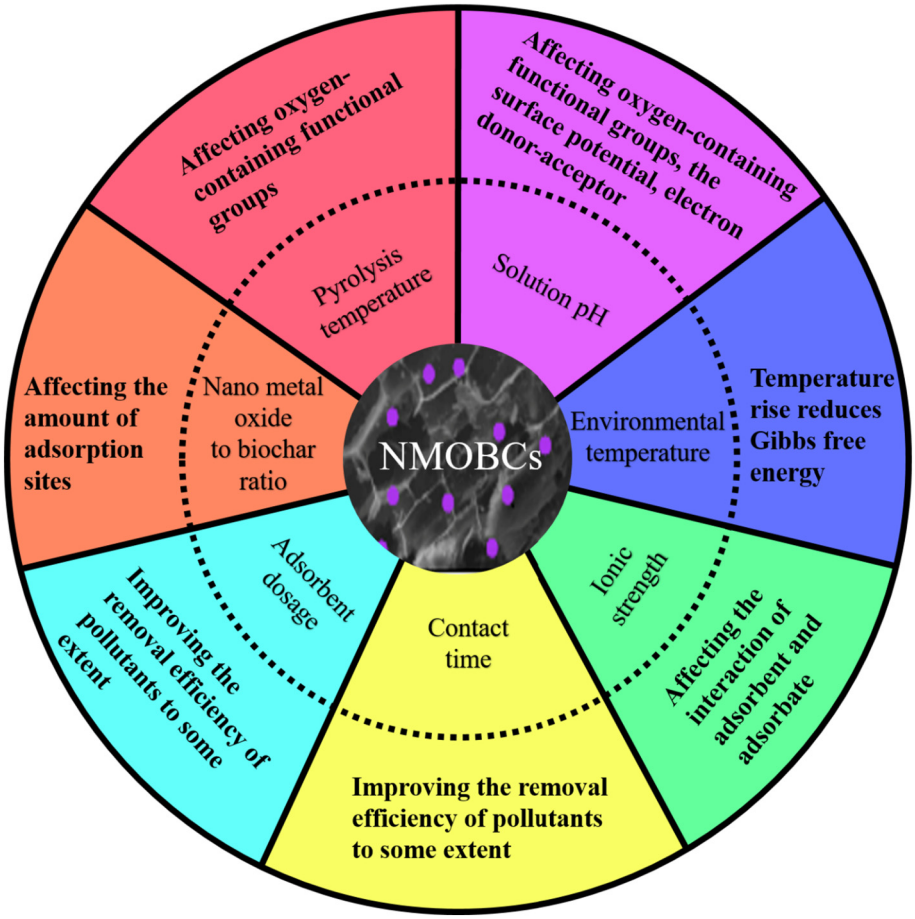

Fig. 3. Possible factors influencing the removal of pollutants by NMOBCs.

NMOBCs decreases as solution pH increases. Moreover, solution pH also has a significant effect on the adsorption of phosphorus by NMOBCs, reaching a maximum at about pH 3.0 (Peng et al., 2020). In summary, the different charge of NMOBCs directly affects their adsorption capacity on different types of pollutants.

3.2. Ambient temperature

The ambient temperature can also affect pollutants adsorption by NMOBCs. The majority of adsorption experiments are conducted at room temperature (25 °C) to simulate the temperature prevalent in polluted environments (Gao et al., 2018; Xu et al., 2018; Xu et al., 2019). Jung et al. (2018) reported that adsorption of Cu(II) by MnO_2-biochar, over a range of 15–45 °C, has been increased with temperature, which is regarded as an indicative of an endothermic process. On the other hand, pollutant adsorption to the nano Fe-Mn oxide-biochar composite, prepared by Zhou et al. (2018), was hardly affected by temperature because the heat was released during the process. Moreover, the pollutant adsorption to the composite of nano-Fe_2O_3 with mushroom waste biochar has been increased with a rise in temperature up to 30 °C (Wang et al., 2019b). A rise in temperature (over a certain range) is conducive to adsorption by lowering the Gibbs free energy (Zhu et al., 2020b), accelerating molecular movement, and promoting adsorbent-ion interaction (Wang et al., 2019b). Therefore, higher ambient temperatures are more favorable for the adsorption process of pollutants by most NMOBCs.

3.3. Ionic strength

The ionic strength of solutions also affects the adsorption capacity of NMOBCs. Coexisting ions in solution can compete with the pollutants for adsorption sites on NMOBCs. Li et al. (2018b), for example, observed that adsorption of fluoroquinolones (FQs) to magnetic MnO_2-biochar composite has been decreased with an increase in ionic strength. This finding was ascribed to the binding of chloride in FQs to cations in solution, inhibiting effective contact between FQs and adsorbent surface. Similarly, Guo et al. (2019) reported that the capacity of ternary HA/Fe-Mn oxide/biochar composite for adsorbing Cd(II) decreased with an increase in ionic strength. It is suggested that Cd(II) was adsorbed by electrostatic interactions. By contrast, the adsorption of As(V) increased with ionic strength, indicative of a covalent binding mechanism. Zhou et al. (2017) also found that surface charge density and surface alkalinity influenced the adsorption of Cu(II) by pristine biochar. In the case of modified biochar, adsorption was controlled by electrostatic attraction between the negatively charged surface sites and positively charged metal ions. Jung et al. (2018) proposed that an increase of salt concentration at the solid-liquid interface could significantly weaken electrostatic interactions between adsorbents and adsorbates, reducing competition between cations in solution and heavy metals. Thus, a low ionic strength is generally conducive to the adsorption of cationic pollutants.

3.4. Other influencing factors

Besides the aforementioned factors, sorbent dosage (Gao et al., 2018; Lian et al., 2019), contact time (Li et al., 2018b), and pyrolysis temperature also influence pollutants adsorption (Feng et al., 2017; Wang et al., 2016). Using nano-MnO_2 modified biochar, Zhu et al. (2020c) obtained the optimal removal of copper citrate from wastewater when the adsorbent dosage was 1.0 g/L. When this dosage was progressively raised, the total number of active sites available for pollutant adsorption increased, as well as the rate of pollutant removal. However,

when the adsorbent dosage exceeded the optimal level, the amount of pollutants removed per unit adsorbent have been decreased (Shen et al., 2020). In consideration of saving cost, the proper sorbent dosage of NMOBCs should be selected especially when they are applied on a large scale.

The pyrolysis temperature of NMOBCs may affect the adsorption of pollutants. The majority of studies show that pollutants adsorption by biochar composites increases with pyrolysis temperature. It may be due to the higher pH and SSA of biochar at higher pyrolysis temperatures (Shen et al., 2019). Feng et al. (2017) found that pyrolysis at highly elevated temperatures of biomass had a depressing effect on the adsorption, probably because of the resultant decrease in the number of functional groups on the composite surface, or even their elimination (Qian et al., 2016). Furthermore, hydroxyl radicals are converted to conjugated aromatic structure-related functional groups with the rise in pyrolysis temperature (Xu et al., 2020b). On the contrary, biochar pyrolyzed at lower temperatures has less porosity and SSA (Hassan et al., 2020). However, it retains more functional groups (Li et al., 2017; Zhao et al., 2018). Therefore, it is necessary to choose a suitable temperature to pyrolyze NMOBCs according to different requirements.

The proportion of nano-metal oxides could also affect the number of adsorption sites on NMOBCs, thereby affecting the adsorption capacity of pollutants. Lin et al. (2019) divided biochar, $FeSO_4 \cdot 7H_2O$ and $KMnO_4$ in different proportions to obtain the optimal ratio of nano-metal oxides to biochar. For the same dosage and concentration of adsorbent, the rate of pollutant removal reached a maximum (96.2%) for the composite prepared at a ratio biochar: $FeSO_4$: $KMnO_4$ of 18: 3: 1. Similarly, the capacity of MgO-modified biochar for removing phosphorus increased with the Mg content of the composite, presumably because MgO served as the main adsorption sites. However, the removal rate decreased when the Mg content exceeded a certain level, probably because the formation of MgO nanoparticles on the surface limited the SSA of the composite (Zhu et al., 2020a).

To evaluate the approximate contributions from different influencing factors, we statistically analyzed the results from 78 studies on the influencing factors and found that 82% of these are concerned with the pH effect, 55% with composite dosage, 38.5% with ionic strength, and 9% with ambient temperature. It would therefore appear that pH is the most important factor influencing pollutants adsorption by NMOBCs (Fig. 4).

4. Mechanisms of pollutants removal by NMOBCs

Generally, the removal of pollutants by NMOBCs depends on physical or chemical effects. Fig. 5 shows the variety of mechanisms that may be involved in the removal of pollutants by NMOBCs. The applications and capacity of different NMOBCs for removing organic and inorganic pollutants are shown in Fig. 6.

4.1. Organic pollutants

The preparation of different NMOBCs and their use as adsorbents of various organic pollutants are summarized in Table 2, meanwhile, the range of mechanisms underlying the adsorption of organic pollutants by NMOBCs is shown in Fig. 5.

4.1.1. Antibiotics

Globally, the increase in antibiotic resistance is a threat to public health in the world (Cheng et al., 2021). The presence of antibiotics in wastewater effluents, discharging into rivers, is also of concern to aquatic animals and living biota (Zhou et al., 2009). Antibiotic resistance genes in soil have been shown to enter the food chain (Chen et al., 2018), and multiple antibiotics have been detected in pork (Shao et al., 2005). Pollution of the environment by antibiotics is seriously affecting the health and safety of human beings and other organisms. Common methods of removing antibiotics in water include adsorption (Ahmed et al., 2015), membrane technology, photocatalytic degradation (Madikizela et al., 2020), uptake by constructed wetlands (Chen et al., 2019), and advanced oxidation (Wang and Zhuan, 2020).

Because of its high efficiency, low cost, and simple operation, adsorption is a widely used method for removing pollutants (Ahmad et al., 2014). Common adsorbents include biochar, carbon nanotubes, graphite, activated carbon, and bentonite (Ahmed et al., 2015). Thus, nano-MnO_2 modified biochar (nMnO_2-BC), prepared by improved coprecipitation, can remove di-*n*-butyl phthalate (DBP) and OTC (Gao et al., 2018). Similarly, magnetic biochar-based MnO_2 composite (MMB), prepared by impregnation, is effective in removing FQs (Li et al., 2018b). Raising the MnO_2 content increases the concentration of oxygen-containing functional groups on the composite surface. Simultaneously, the SSA of the composite decreases due to blockage of surface pores by spherical nanoparticles of MnO_2. X-ray photoelectron spectroscopy (XPS) analysis indicated that adsorption of DBP or OTC by nMnO_2-BC was accompanied by partial reduction of Mn(IV) to Mn(III) and Mn(II), accelerating the oxidative degradation of DBP and OTC. Being unsaturated, the molecules of DBP and OTC can act as π-electron acceptors (Gao et al., 2018). At the same time, the biochar-based graphite-like structure can function as a π donor, enabling π-π interactions to occur. The maximum adsorption capacity of MMB for norfloxacin, ciprofloxacin, and enrofloxacin of 6.94, 8.37, and 7.19 mg/g was respectively 1.2, 1.5 and 1.6 times higher than those of pristine

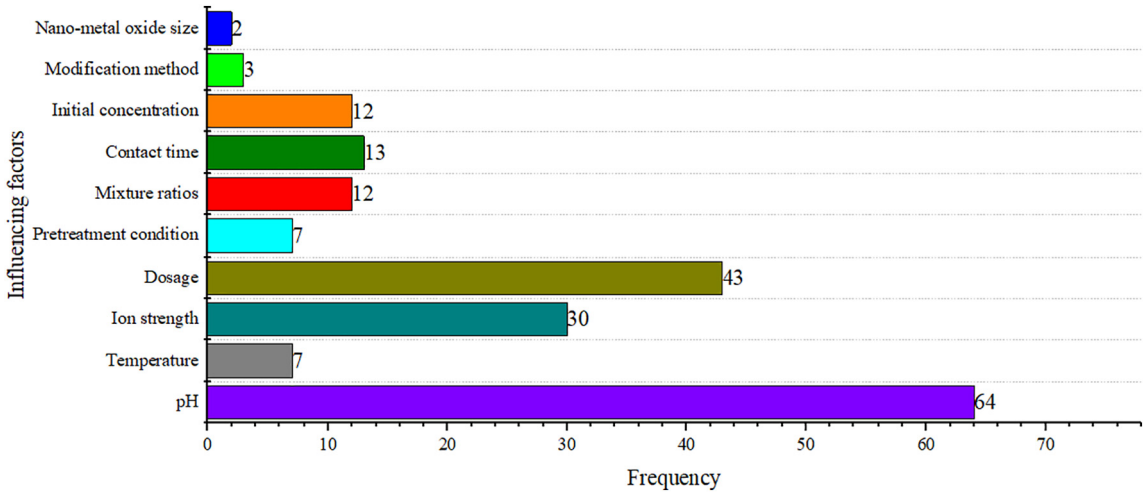

Fig. 4. Relative importance of different factors influencing pollutants adsorption by NMOBCs (data from 78 studies).

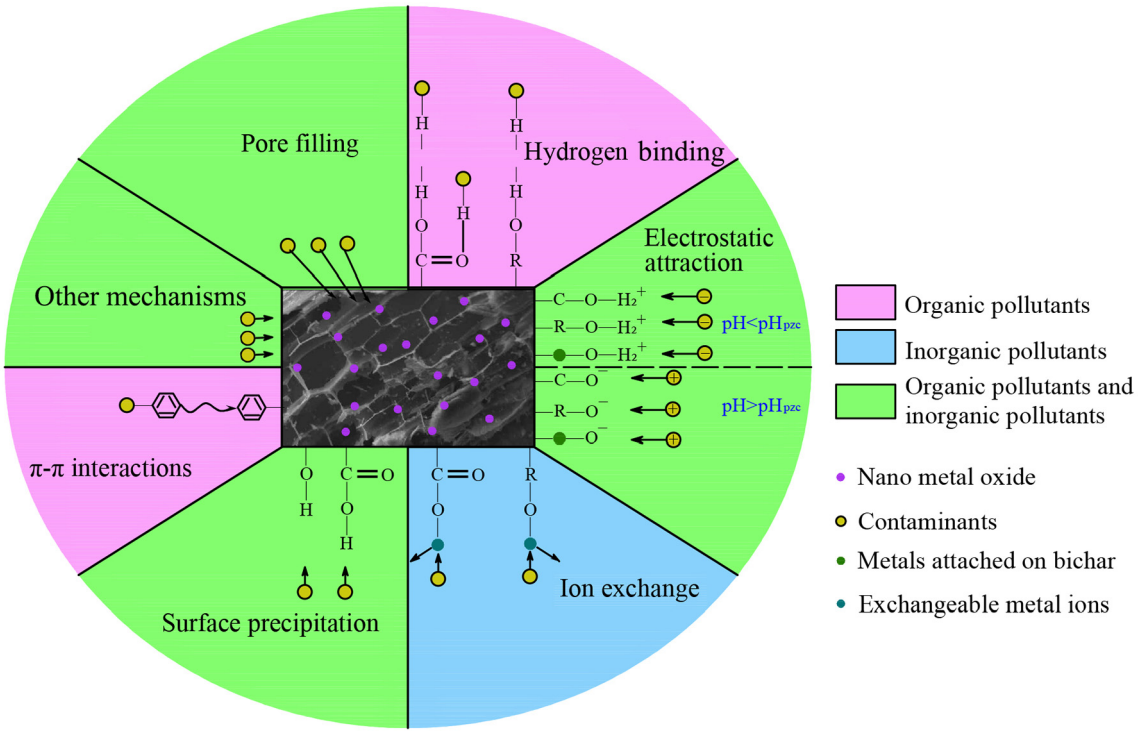

Fig. 5. Possible removal mechanisms of pollutants by NMOBCs.

biochar. The adsorption process was spontaneous and endothermic, while adsorption decreased with an increase in solution pH (3.0–10.0) and ionic strength (0.001–0.1) (Li et al., 2018b). Meanwhile, Shen et al. (2020) also used nano-MnO_2-biochar composite to remove tetracycline and found that the adsorption capacity was 131.49 mg/g, greater than that of FQs. Biochar loaded with nano-ZnO composites were also used to remove antibiotics. Gholami et al. (2019) impregnated biochar with nanoparticles of ZnO and used the composite to degrade gemifloxacin. The rod-shaped ZnO particles of 20–40 nm diameters were randomly distributed, giving rise to a composite with a high SSA and porosity. Following 45 min of ultrasonic irradiation, the composite could degrade 96.1% of gemifloxacin at a concentration of 20.0 mg/L, pH 5.5, in the presence of 1.5 g/L ZnO-biochar. Gemifloxacin was first decomposed into aromatic and aliphatic intermediates, and then mineralized into CO_2, H_2O, and inorganic ions.

After loading nano-metal oxides, the surface charges of NMOBCs change from negative to positive, thereby enhancing the adsorption of anionic pollutants, and also provide oxygen-containing functional groups (Krasucka et al., 2021). In general, the adsorption mechanisms of NMOBCs for antibiotics can be mainly summarized as redox and π-π interactions.

4.1.2. Organic dyes

The widespread use of dyes in many industries has led to serious pollution of the associated wastewater, and hence affects human health and the growth of aquatic plants and other living organisms (Adegoke and Bello, 2015). Several methods were used for the removal of dyes, such as adsorption (Bharathiraja et al., 2019), membrane technology (Wu et al., 2020a), advanced oxidation, electrochemical process, and biodegradation (Zhou et al., 2019). Among them, adsorption is the most commonly used method due to its simplicity, low cost, and high efficiency (Mu and Wang, 2016).

Due to the different surface charges of dye molecules, the adsorption capacity of NMOBCs on dyes may be varied. Using pulp and pulp sludge as feedstocks, Chaukura et al. (2016) prepared nano-Fe_2O_3-biochar composite by impregnation for the adsorption of methyl orange. The SSA of the composite was far lower than that of pristine biochar, indicating that nano-Fe_2O_3 occupied the interstitial pores of biochar. FTIR analysis showed that cationic methyl orange may form ionic interactions with hydroxyl, carboxyl functional groups and electron dense double bonds in addition to dative bonds in the composite. The adsorption process was spontaneous, showing a maximum of 20.53 mg/g at a contact time of 30 min and pH 8.0. Goncalves et al. (2020) also used nano-ZnO-biochar composite to degrade methyl orange, but obtained only 4.515 mg/g. Khataee et al. (2017) used biochar loaded with nano-ZrO_2 particles (5–40 nm diameters) to degrade Reactive Yellow 39 dyes ultrasonically. The total pore volume and SSA of the composite were higher than the corresponding values of pristine biochar. A degradation rate of 96.8% was obtained at a composite dosage of 1.5 g/L, pH 6.0, an initial dye concentration of Reactive Yellow 39 was 20.0 mg/L, and an ultrasonic power of 300 W. The degradation of Reactive Yellow 39 involved the destruction of C-S, C-Br, C-N, N-N and C-C bonds to yield amides and carboxylic acids with a low carbon content which were then completely mineralized. Generally, both electrostatic attraction and chelation could contribute to the adsorption of organic dyes by NMOBCs (Jung et al., 2016; Zhang et al., 2020d).

4.1.3. Other organic pollutants

NMOBCs have not only been used to adsorb and remove organic pollutants other than those mentioned above but also can activate persulfate (PS) to improve the removal rate of organic pollutants. For instance, nano-CuO-biochar composite (CuO/BC), prepared by the hydrothermal method, can degrade BPA in combination with PS (Luo et al., 2019). The CuO/BC-PS system could completely degrade BPA by transferring electrons from the pollutant to PS through an intermediate formed by the combination reaction between CuO/BC and PS. Ouyang et al. (2017) prepared a nano-Fe_3O_4-biochar composite by impregnation and used it to activate PS and degrade 1,4-dioxane. The spherical nano-Fe_3O_4 particles were uniformly distributed on the biochar surface. At room temperature and neutral pH, the composite could degrade 98% of 1,4-dioxane in polluted water. XPS analysis showed that the oxygen functional groups on the surface of the biochar and the ferrous ions activate the PS, which may improve the degradation efficiency of the composite.

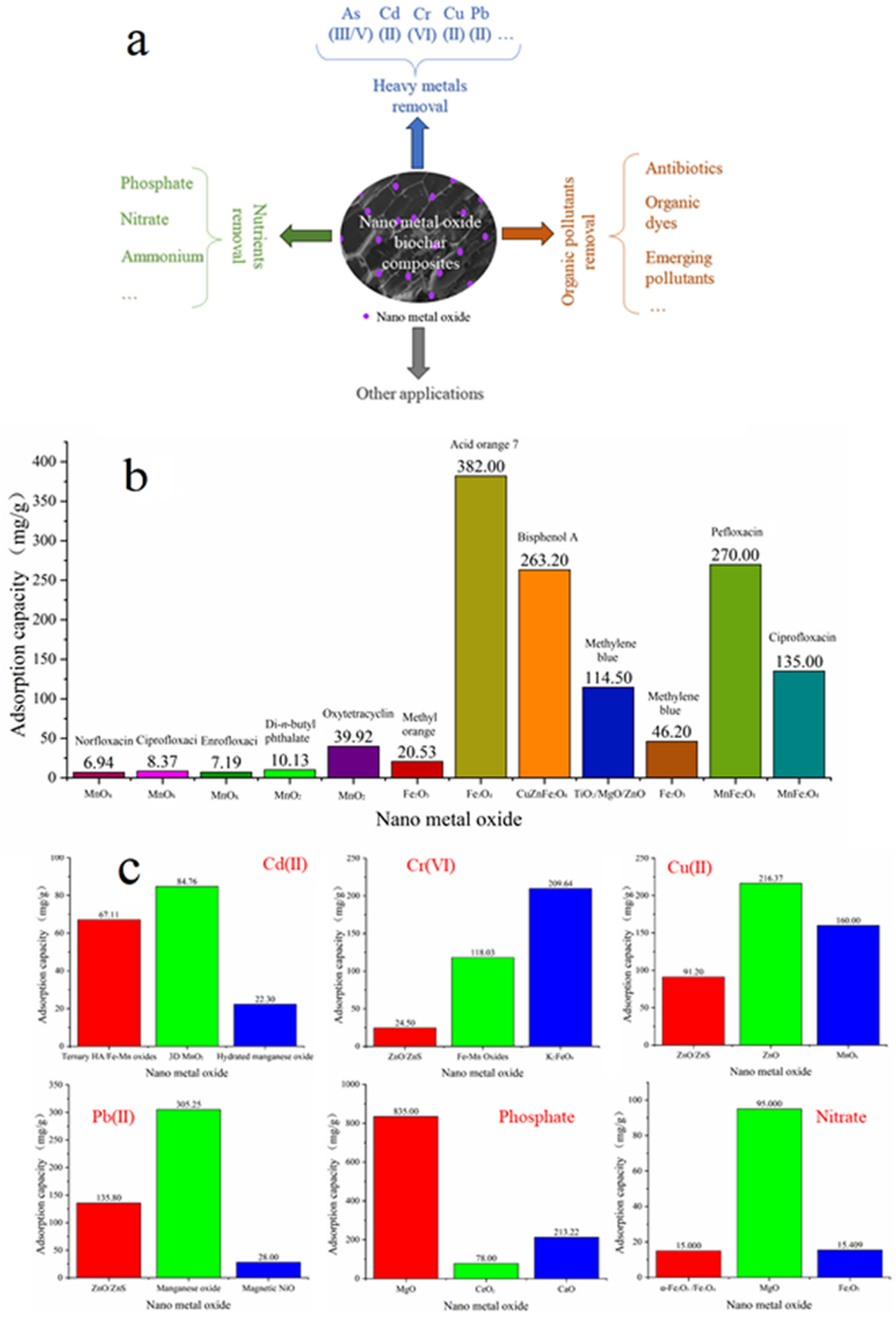

Fig. 6. (a) Applications of NMOBCs for pollutants removal; (b) Comparison of adsorption capacity of different NMOBCs with respect to organic pollutants; (c) Comparison of adsorption capacity of different NMOBCs with respect to inorganic pollutants.

Table 2
Preparation and properties of some NMOBCs for adsorbing various organic pollutants.

Feedstocks	Metal oxides	Pyrolysis temperature (°C)	Residence time (min)	Solution pH	Adsorbates	Adsorption capacity (mg/g)	Adsorption model	References
Potato stems and leaves	MnO_x	500	30	6.0	Norfloxacin	6.94	Langmuir	(Li et al., 2018b)
Potato stems and leaves	MnO_x	500	30	6.0	Ciprofloxacin	8.37	Langmuir	(Li et al., 2018b)
Potato stems and leaves	MnO_x	500	30	6.0	Enrofloxacin	7.19	Langmuir	(Li et al., 2018b)
Corn stalks	MnO_2	600	120	7.0	Di-*n*-butyl phthalate	10.13	Langmuir	(Gao et al., 2018)
Corn stalks	MnO_2	600	120	7.0	Oxytetracycline	39.92	Langmuir	(Gao et al., 2018)
Wheat husks and paper sludge	ZnO	500	20	5.5	Gemifloxacin	13.33	N.A.	(Gholami et al., 2019)
Paper and pulp sludge	Fe_2O_3	750	30	8.0	Methyl orange	20.53	Freundlich	(Chaukura et al., 2016)
Brown marine macroalgae	Fe_3O_4	600	60	5.0	Acid orange 7	382.00	Sips	(Jung et al., 2016)
Bamboo	$CuZnFe_2O_4$	550	60	3.0	Bisphenol A	263.20	Langmuir	(Heo et al., 2019)
Bamboo	TiO_2/MgO/ZnO	700	60	N.S.	Methylene blue	114.50	Langmuir	(Zhai et al., 2019)
Pine needles	$MnFe_2O_4$	500	120	5.5	Tetracycline	N.D.	N.A.	(Lai et al., 2019)
Peanut shell	Fe_2O_3	400	240	3.0	Methylene blue	46.20	N.A.	(Qiu et al., 2020)
Peanut shell	Fe_2O_3	400	240	3.0	Acid orange 7	N.D.	N.A.	(Qiu et al., 2020)
Sewage sludge	ZnO	450	180	7.0	Acid orange 7	N.D.	N.A.	(Guan et al., 2020)
Vinasse	$MnFe_2O_4$	800	60	5.0	Pefloxacin	270.00	Freundlich	(Xiang et al., 2020)
Vinasse	$MnFe_2O_4$	800	60	5.0	Ciprofloxacin	135.00	Freundlich	(Xiang et al., 2020)
Wheat straw	Co_3O_4	450	240	7.0	Chloramphenicols	600.00	N.A.	(Xu et al., 2020a)

Notes: N.A. = not available; N.D. = not determined.

4.2. Inorganic pollutants

The various mechanisms underlying the adsorption and removal of inorganic pollutants by NMOBCs are shown in Fig. 5.

4.2.1. Heavy metals

Industrial processes keep on discharging toxic heavy metals into the environment, either directly or indirectly. Since heavy metals are not degradable, they tend to accumulate in the environment affecting human health and agricultural production (Beidokhti et al., 2019; Foong et al., 2020). Common methods for removing heavy metals include adsorption (Bai et al., 2020), membrane technology (Foong et al., 2020), precipitation (Kurniawan et al., 2006), and electrochemical methods (Heidmann and Calmano, 2008). In this regard, NMOBCs as adsorbents have been the method of choice because of their low cost and high efficiencies (Table 3).

More and more studies have been used nano-MnO_2 modified biochar to remove different heavy metals. Zhou et al. (2017) used a nano-MnO_2-biochar composite (NMBC), prepared by impregnation, to remove Cu(II) from aqueous solution. The spherical MnO_2 nanoparticles formed dense clusters of about 30 nm diameters over the entire biochar surface. The capacity of NMBC for adsorbing Cu(II) increased with pH (3.0 to 6.0) but was not affected by solution ionic strength. Following its adsorption to NMBC, Cu(II) was transformed to CuO, $Cu(C_2H_3O_2)_2$, and $Cu(OH)_2$, indicating that precipitation and chelation play an important role in the adsorption process which is spontaneous and endothermic. Similarly, the MnO_2-biochar composite (FMBC) of Zhou et al. (2018), prepared by impregnation, could adsorb Cu(II) and Cd(II) in sewage. FMBC had a lower carbon content but higher surface oxygen,

Table 3
Preparation and properties of some NMOBCs for adsorbing various heavy metals.

Feedstocks	Metal oxides	Pyrolysis temperature (°C)	Residence time (min)	Solution pH	Adsorbates	Adsorption capacity (mg/g)	Adsorption model	References
Corn straw	Fe-Mn oxides	600	30	6.0	Cd(II)	101.00	Langmuir	(Zhou et al., 2018)
Rice husks	Ternary HA/Fe-Mn oxides	500	180	8.0	Cd(II)	67.11	Freundlich	(Guo et al., 2019)
Rice husks	3D MnO_2	500	120	6.0	Cd(II)	84.76	Langmuir	(Wu et al., 2020b)
Peanut shell	Hydrated manganese oxide	400	60	5.0	Cd(II)	22.30	Freundlich	(Wan et al., 2018)
Corn stover	ZnO/ZnS	600	60	9.0	Cr(VI)	24.50	Freundlich	(Li et al., 2018a)
Corn stover	Fe-Mn Oxides	400	120	2.0	Cr(VI)	118.03	Langmuir	(Zhu et al., 2020b)
Pomelo peel	K_2FeO_4	300	60	2.0	Cr(VI)	209.64	Langmuir	(Yin et al., 2020)
Corn stover	ZnO/ZnS	600	60	9.0	Cu(II)	91.20	Freundlich	(Li et al., 2018a)
Waste pomelo peel	ZnO	800	60	5.0	Cu(II)	216.37	Langmuir	(Wang et al., 2019e)
Corn straw	MnO_x	600	30	6.0	Cu(II)	160.00	Langmuir	(Song et al., 2014)
Corn straw	MnO_2	600	30	7.0	As(III)	14.36	Langmuir	(Yu et al., 2015)
Corn stem powder	Fe-Mn Oxides	600	120	3.0	As(III)	8.80	Freundlich	(Lin et al., 2019)
Rice husks	Ternary HA/Fe-Mn oxides	500	180	3.0	As(V)	35.59	Freundlich	(Guo et al., 2019)
Corn stover	ZnO/ZnS	600	60	9.0	Pb(II)	135.80	Freundlich	(Li et al., 2018a)
Rice straws	Manganese oxide	420	240	5.0	Pb(II)	305.25	Langmuir	(Tan et al., 2018)
Prosopis juliflora wood pieces	Magnetic NiO	400	120	6.0	Pb(II)	28.00	Langmuir	(Saravanakumar et al., 2019)
Rice husks	3D MnO_2	500	120	4.0	Pb(II)	70.90	Langmuir	(Wu et al., 2020b)
Rice husks	MnO_x	800	20	5.0	Pb(II)	86.50	Langmuir	(Faheem et al., 2016)
Peanut shell	Hydrated manganese oxide	400	60	5.0	Pb(II)	67.90	Freundlich	(Wan et al., 2018)

iron and manganese content than pristine biochar, indicating the presence of a large number of highly polar oxygen-containing functional groups. An increase in pH (4.0–6.0) and a high humic acid concentration were conducive to Cu(II) and Cd(II) adsorption during which carboxyl groups were consumed and strong monodentate or multidentate inner balls of Mn-O-M were formed. XPS analysis showed that Cu(II), adsorbed on the surface of FMBC, formed CuO, $CuCO_3$, and $Cu(OH)_2$, while Cd(II) existed in the form of $Cd(OH)_2$ and CdO. Cation-π interactions might also be involved in the adsorption of Cu(II) and Cd(II). Hierarchical birnessite-type MnO_2-biochar composite, synthesized by a hydrothermal process, could remove Cu(II) from polluted water (Jung et al., 2018). Adsorption kinetics and isotherms indicated that diffusion into membranes and pores, physical adsorption, and endothermic mechanisms were involved in the removal of Cu(II) from solution. The nano-MnO_2 modified biochar composite that Yu et al. (2015) prepared, was a good adsorbent of As(III) in red soil. The deposition of nano-MnO_2 particles in the pores of biochar led to a sharp decrease in the SSA of the composite. Fourier transform infrared spectrometry (FTIR) and XPS analysis showed that As(III) interacted with oxygen-containing functional groups forming Mn-O/As and Fe-O/As bonds. Adsorbed As(III) was also partially oxidized to As(V) by MnO_2 and Fe-Mn oxide.

Biochar loaded with nano-Fe_xO_y showed high removal efficiency for Cr(VI). Liu et al. (2019) used nano-Fe_2O_3-biochar composite to remove Cr(VI). The α-Fe_2O_3 nanoparticles, with diameters of 20–50 nm, were uniformly distributed on the biochar surface. The adsorption of Cr(VI) (reaching 90% within 1 min) led to the conversion of α-Fe_2O_3 into spherical particles of 100–200 nm diameters, which may be attributed to the formation of $(Cr_xFe_{1-x})(OH)_3$ precipitates. And Cr(VI) adsorption was controlled by the amount of α-Fe_2O_3 through electrostatic attraction. Subsequently, the maximum removal rate of Cr(VI) for the nano-Fe_3O_4-biochar composite, prepared by Wang et al. (2019b), reached 99.44%, while the removal efficiency was maintained at 78.56% after 7 cycles of regeneration. The high affinity of this composite's nanostructures for Cr(VI) is conducive to adsorption. Furthermore, Fe_3O_4 could reduce Cr(VI), while the formation of surface complexes between –CH, –OH, –COOH, and FeO also contributed to Cr(VI) adsorption.

Nano Fe-Mn polynary oxides modified biochar is also used to immobilize heavy metals. Fe-Mn oxide-biochar, prepared by impregnation, was used by Lin et al. (2019) to adsorb As from aqueous solutions. FTIR and XPS analysis showed that As(III) was oxidized to As(V) on the surface of Fe- and Mn-oxide particles. As(V) was preferentially adsorbed to As(III), forming As-O bonds on the Fe-Mn oxide surface. Following adsorption, the surface of the composite became concave and uneven due to the filling of the micropores by Fe- or Mn- oxide, leading to a reduction in SSA. The maximum adsorption capacity for As(III) was 8.8 mg/g. However, nano Fe-Mn binary oxide–biochar produced by Zhou et al. (2018) showed better adsorption capacity for Cd(II), which was 101.0 mg/g, about 11 times higher than that of Lin et al. (2019). A new composite of biochar with ternary HA/Fe-Mn oxide (HFMB), prepared by impregnation, was used by Guo et al. (2019) to adsorb Cd(II) and As(V). HFMB had a flower-like structure composed of MnO_2, exposing a high SSA and a large number of sites to which Cd(II) and As (V) could adsorb. Compared with the unmodified biochar, the composite had a highly enlarged pore volume, enabling Cd(II) and As(V) to enter the internal pore system. XPS and FTIR indicated the chelation of Cd(II) to HFMB, and the formation of CdO, $CdCO_3$, and $Cd(OH)_2$ while in the case of As(V), ligand exchange was the controlling mechanism.

At the same time, biochar loaded with nano-ZnO was used to remove heavy metals. Li et al. (2018a) used nano-ZnO/ZnS modified biochar, prepared by direct pyrolysis, to remove Pb(II), Cu(II), and Cr (VI) from solution. The ZnO/ZnS-modified biochar had a larger SSA (397.4 m^2/g) and porosity (total pore volumes = 0.43 cm^3/g) than the pristine biochar (SSA = 102.9 m^2/g; total pore volumes = 0.2 cm^3/g). The carbon matrix played an important role in the adsorption process. The hydroxyl groups on the nano-ZnO/ZnS surface could complex heavy metals, while the cations could exchange with their heavy metal counterparts. Similarly, Yu et al. (2018) were able to remove Cr(VI) in an aqueous solution, using biochar impregnated with ZnO nanoparticles. The ZnO particles with diameters of 13–60 nm were uniformly distributed on the biochar surface. The composite with a 30 wt% loading of ZnO could remove up to 95% of Cr(VI), showing a 70% removal rate at the fifth cycle. The impregnated ZnO could catalyze the formation of hydrated Zn-Cr oxide complexes as well as the reduction of Cr(VI) to Cr(III).

In general, both physisorption and chemisorption affect the adsorption process of heavy metals by NMOBCs. Physisorption mainly includes pore filling and electrostatic attraction. Meanwhile, chemisorption mainly includes chelation, complexation, deposition, ion and ligand exchange, redox and surface precipitation. Among them, chemisorption predominates the adsorption process. The relative importance of these processes is dependent on the type and valency of the targeted heavy metals. Due to the good performance and universal applicability, there will be more studies on using nano-MnO_2, ZnO and Fe_xO_y to modified biochar in the future.

4.2.2. Nutrients

Excess nutrients can lead to eutrophication of water (Alzeyadi et al., 2019). A large number of NMOBCs have been used to adsorb nutrients (Table 4), such as phosphate, nitrate, and ammonium, biochar composites with nano-MgO and Fe_2O_3 have taken center stage. This is because nano-MgO modified biochar is positively charged, and hence capable of taking up anionic species through electrostatic attraction and surface precipitation. For example, Xu et al. (2018, 2019) used composites of wood waste biochar with nano-MgO, prepared by impregnation, to remove (and recover) phosphate and ammonium from human urine. Phosphate was removed through electrostatic attraction supplemented by surface adsorption and precipitation. On the other hand, ammonium was removed through the formation and precipitation of struvite on the biochar surface. Subsequently, Zheng et al. (2020) reported the removal of phosphate and methylene blue, using a composite of biochar with ball-milled MgO. The MgO nanoparticles of about 20 nm were evenly and uniformly dispersed in the biochar, increasing its SSA and adsorption capacity. And phosphate adsorption can be attributed to the surface precipitation and electrostatic attraction between anionic phosphate and positively charged MgO surface. Similarly, Zhang et al. (2012) were able to remove phosphate and nitrate in aqueous solutions using porous MgO-biochar nanocomposites. The composite derived from beet pulp and peanut shells and nano-MgO flakes gave the best performance in terms of nutrient adsorption. This observation was ascribed to the even distribution on the biochar surface of MgO flakes of ~ 10–25 nm in thickness and ~ 0.2–1 μm in length. These nanostructures were randomly oriented and grew from the surface of the biochar, giving rise to a nanoporous composite with a large adsorbing surface. Using similar nano-MgO-biochar composites, the phosphorus adsorption capacity of Xu et al. (2018) was 116.4 mg/g, as that of Zhang et al. (2012) reached 835.0 mg/g, about 7 times higher than the former.

Nano-Fe_xO_y modified biochar also showed a good adsorption effect on nutrients. He et al. (2017) loaded a Fe_3O_4-biochar nanocomposite with photosynthetic bacteria (PSB) by chemical coprecipitation and used the material for the bioremediation of wastewater. The Fe_3O_4 nanoparticles were evenly distributed on the biochar matrix, providing extensive SSA and active sites for PSB attachment (5.45×10^9 cells/g). The composite was capable of removing 83.1% chemical oxygen demand, 87.5% NH_4^+, and 92.1% PO_4^{3-} from wastewater. Phosphate was removed by ligand exchange and electrostatic attraction to the positively charged Fe_3O_4. On the other hand, NH_4^+ would be repelled by Fe_3O_4 nanoparticles, limiting uptake. Subsequently, Zhu et al. (2018) obtained a porous composite by impregnating nanoparticles of α-Fe_2O_3/Fe_3O_4 into bamboo biochar. The resultant material (HPA-Fe/C-B) was then used to remove phosphorus in sewage. At an initial phosphorus concentration of 2.0–50.0 mg/L, the amount of P adsorbed increased from 0.20 to 2.46, 2.62, and 2.81 mg/g at 25, 35 and 45 °C, respectively. At an initial

Table 4
Preparation and properties of some NMOBCs for adsorbing various nutrients.

Feedstocks	Metal oxides	Pyrolysis temperature (°C)	Residence time (min)	Solution pH	Adsorbates	Adsorption capacity (mg/g)	Adsorption model	References
Populus X Canadensis Moench and Sophora japonica Linn	MgO	600	N.S.	7.0	Phosphate	118.00	Langmuir	(Xu et al., 2019)
Populus X Canadensis Moench and Sophora japonica Linn	MgO	600	N.S.	8.45	Phosphate	116.40	Langmuir	(Xu et al., 2018)
Sugarcane bagasse, peanut shells mixture	MgO	600	60	N.S.	Phosphate	835.00	Langmuir	(Zhang et al., 2012)
Sugarcane harvest residue	MgO	550	60	4.0	Phosphate	398.00	Langmuir	(Li et al., 2017)
Corn straw	MgO	550	30	6.7	Phosphate	60.95	Langmuir-Freundlich	(Zhu et al., 2020a)
Dewatered sludge	$MnAl_2O_4$	180	720	3.0	Phosphate	28.20	Langmuir	(Peng et al., 2020)
Maize straw	CeO_2	300	100	10.0	Phosphate	78.00	Langmuir	(Feng et al., 2017)
Wheat straw	CaO	600	120	11.0	Phosphate	213.22	Langmuir-Freundlich	(Li et al., 2020c)
Bamboo	α-Fe_2O_3/Fe_3O_4	600	180	3.0	Phosphate	2.81	Langmuir	(Zhu et al., 2018)
Douglas fir	α-Fe_2O_3/Fe_3O_4	600	60	2.0	Nitrate	15.00	Langmuir	(Dewage et al., 2018)
Corn straw	Fe_2O_3	550	30	N.S.	Nitrate	15.409	Langmuir	(Li et al., 2020b)
Sugarcane bagasse, peanut shells mixture	MgO	600	60	N.S.	Nitrate	95.00	Langmuir	(Zhang et al., 2012)

Notes: N.S. = not specified.

phosphorus concentration of 2.0, 5.0, and 10.0 mg/L, the maximum removal rate of phosphorus was 99.2%, 97.5%, and 84.4%, respectively. According to the results mentioned above, the maximum removal rate of phosphorus reached >90%, indicating that nano-Fe_xO_y modified biochar has a good phosphorus removal efficiency.

Nano-Ce_2O functionalized biochar (Ce-MSB), prepared by impregnation, was used by Feng et al. (2017) to remove, or retain phosphorus in soil. Application of Ce-MSB to a paddy soil column reduced the total P concentration of surface water by 27.33% while increasing the total P content of the surface soil by 7.22%. Based on the assumption of Ho's pseudo-second kinetic model, the adsorption of phosphate by Ce-MSB was attributed to chemisorption.

Generally, the results from the above studies on different NMOBCs suggest that electrostatic attraction, surface precipitation and ligand exchange are the potential mechanisms of nutrients adsorption by NMOBCs. Further studies are needed to identify the main mechanisms.

5. Conclusions and future perspectives

The present review is concerned with the preparation of NMOBCs, the factors influencing the adsorption of environmental pollutants to NMOBCs, and the underlying adsorption mechanisms. NMOBCs not only have effective performance on removing various pollutants from solution, but also are economical to produce and are recyclable. NMOBCs will receive more attention in the future due to its superiority. However, the following issues need to be considered before their large-scale application.

Firstly, due to nano-metal oxides contain metal elements, it is necessary to assess the stability, recyclability comprehensively, and environmental risks of NMOBCs. Secondly, because of their small particle sizes, NMOBCs are readily dispersible in, also difficult to separate from polluted water. Future researches should, therefore, focus on developing effective methods of isolating NMOBCs from the reaction mixture for subsequent processing. In this regard, the magnetization of the composites is worth investigating as does embedding, crosslinking, or loading the composites with other nanoparticulate reagents (Wang et al., 2018c). Thirdly, most of the work on pollutants removal by NMOBCs has been done using aqueous solutions and batch experiments. The latter approach needs to be extended to the pilot scale before applying NMOBCs for the remediation of actual contaminated sites, such as discharged industrial wastewater. Equally important is to develop large-scale, cost-effective, environmentally friendly methods of preparing NMOBCs for the removal of emerging and complex compound pollutants (Liu et al., 2020; Zhang et al., 2020c). Finally, the risk to the environment, and associated hazards to organisms, posed by the application of NMOBCs to clean up polluted water and soil, need to be kept in mind.

Declaration of competing interest

The authors declare that they have no known competing financial interests or personal relationships that could have appeared to influence the work reported in this paper.

Acknowledgements

This work was supported by the National Key Research and Development Program of China (2016YFC0502602), the National Natural Science Foundation of China (41977297), the High-Level Overseas Talent Innovation and Entrepreneurship Project of Guizhou Province [(2018)08], and the Special Research Fund for Natural Science (Special Post) of Guizhou University [(2020)01].

References

Adegoke, K.A., Bello, O.S., 2015. Dye sequestration using agricultural wastes as adsorbents. Water Resources and Industry 12, 8–24. https://doi.org/10.1016/j.wri.2015.09.002.

Ahmad, M., Rajapaksha, A.U., Lim, J.E., Zhang, M., Bolan, N., Mohan, D., et al., 2014. Biochar as a sorbent for contaminant management in soil and water: a review. Chemosphere 99, 19–33. https://doi.org/10.1016/j.chemosphere.2013.10.071.

Ahmed, M.B., Zhou, J.L., Ngo, H.H., Guo, W., 2015. Adsorptive removal of antibiotics from water and wastewater: progress and challenges. Sci. Total Environ. 532, 112–126. https://doi.org/10.1016/j.scitotenv.2015.05.130.

Ahmed, M.B., Zhou, J.L., Ngo, H.H., Guo, W., Chen, M., 2016. Progress in the preparation and application of modified biochar for improved contaminant removal from water and wastewater. Bioresour. Technol. 214, 836–851. https://doi.org/10.1016/j.biortech.2016.05.057.

Ali, S., Rizwan, M., Noureen, S., Anwar, S., Ali, B., Naveed, M., et al., 2019. Combined use of biochar and zinc oxide nanoparticle foliar spray improved the plant growth and decreased the cadmium accumulation in rice (*Oryza sativa L.*) plant. Environ. Sci. Pollut. Res. 26, 11288–11299. https://doi.org/10.1007/s11356-019-04554-y.

Alzeyadi A, Al-Ansari N, Laue J, Alattabi A, 2019. Study of biomass bottom ash efficiency as phosphate sorbent material. Civil Engineering Journal 5, 2392–2401. doi:10.28991/cej-2019-03091419.

Bai, S., Wang, L., Ma, F., Zhu, S., Xiao, T., Yu, T., et al., 2020. Self-assembly biochar colloids mycelial pellet for heavy metal removal from aqueous solution. Chemosphere 242, 125182. https://doi.org/10.1016/j.chemosphere.2019.125182.

Beidokhti MZ, Naeeni STO, AbdiGhahroudi MS, 2019. Biosorption of nickel (II) from aqueous solutions onto pistachio Hull waste as a low-cost biosorbent. Civil Engineering Journal 5, 447–457. doi:10.28991/cej-2019-03091259.

Bharathiraja, B., Ebenezer Selvakumari, I.A., Iyyappan, J., Varjani, S., 2019. Itaconic acid: an effective sorbent for removal of pollutants from dye industry effluents. Current Opinion in Environmental Science & Health 12, 6–17. https://doi.org/10.1016/j.coesh.2019.07.004.

Bhateria, R., Singh, R., 2019. A review on nanotechnological application of magnetic iron oxides for heavy metal removal. Journal of Water Process Engineering 31, 100845. https://doi.org/10.1016/j.jwpe.2019.100845.

Cha, J.S., Park, S.H., Jung, S.-C., Ryu, C., Jeon, J.-K., Shin, M.-C., et al., 2016. Production and utilization of biochar: a review. J. Ind. Eng. Chem. 40, 1–15. https://doi.org/10.1016/j.jiec.2016.06.002.

Chaukura, N., Murimba, E.C., Gwenzi, W., 2016. Synthesis, characterisation and methyl orange adsorption capacity of ferric oxide–biochar nano-composites derived from pulp and paper sludge. Appl Water Sci 7, 2175–2186. https://doi.org/10.1007/s13201-016-0392-5.

Chen, Q., Fan, X., Zhu, D., An, X., Su, J., Cui, L., 2018. Effect of biochar amendment on the alleviation of antibiotic resistance in soil and phyllosphere of *Brassica chinensis* L. Soil Biol. Biochem. 119, 74–82. https://doi.org/10.1016/j.soilbio.2018.01.015.

Chen, M., Zhu, M., Zhu, Y., Wang, D., Li, Z., Zeng, G., et al., 2019. Collision of emerging and traditional methods for antibiotics removal: taking constructed wetlands and nanotechnology as an example. NanoImpact 15, 100175. https://doi.org/10.1016/j.impact.2019.100175.

Cheng, N., Wang, B., Wu, P., Lee, X., Xing, Y., Chen, M., et al., 2021. Adsorption of emerging contaminants from water and wastewater by modified biochar: a review. Environmental Pollution, 116448 https://doi.org/10.1016/j.envpol.2021.116448.

Dasgupta, N., Ranjan, S., Ramalingam, C., 2017. Applications of nanotechnology in agriculture and water quality management. Environ. Chem. Lett. 15, 591–605. https://doi.org/10.1007/s10311-017-0648-9.

Dewage, N.B., Liyanage, A.S., Pittman, C.U., Mohan, D., MIsna, T., 2018. Fast nitrate and fluoride adsorption and magnetic separation from water on α-Fe_2O_3 and Fe_3O_4 dispersed on Douglas fir biochar. Bioresour. Technol. 263, 258–265. https://doi.org/10.1016/j.biortech.2018.05.001.

Faheem, Yu H., Liu, J., Shen, J., Sun, X., Li, J., et al., 2016. Preparation of MnO_x-loaded biochar for Pb^{2+} removal: adsorption performance and possible mechanism. J. Taiwan Inst. Chem. Eng. 66, 313–320. https://doi.org/10.1016/j.jtice.2016.07.010.

Feng, Y., Lu, H., Liu, Y., Xue, L., Dionysiou, D.D., Yang, L., et al., 2017. Nano-cerium oxide functionalized biochar for phosphate retention: preparation, optimization and rice paddy application. Chemosphere 185, 816–825. https://doi.org/10.1016/j.chemosphere.2017.07.107.

Foong, C.Y., Wirzal, M.D.H., Bustam, M.A., 2020. A review on nanofibers membrane with amino-based ionic liquid for heavy metal removal. J. Mol. Liq. 297, 111793. https://doi.org/10.1016/j.molliq.2019.111793.

Gao, M., Zhang, Y., Gong, X., Song, Z., Guo, Z., 2018. Removal mechanism of di-*n*-butyl phthalate and oxytetracycline from aqueous solutions by nano-manganese dioxide modified biochar. Environ. Sci. Pollut. Res. 25, 7796–7807. https://doi.org/10.1007/s11356-017-1089-5.

Gharibshahian E, 2020. The effect of polyvinyl alcohol concentration on the growth kinetics of $KTiOPO_4$ nanoparticles synthesized by the co-precipitation method. HighTech and Innovation Journal 1, 187–93. doi:10.28991/HIJ-2020-01-04-06.

Gholami, P., Dinpazhoh, L., Khataee, A., Orooji, Y., 2019. Sonocatalytic activity of biochar-supported ZnO nanorods in degradation of gemifloxacin: synergy study, effect of parameters and phytotoxicity evaluation. Ultrasonics - Sonochemistry 55, 44–56. https://doi.org/10.1016/j.ultsonch.2019.03.001.

Goncalves, M.G., da Silva Veiga, P.A., Fornari, M.R., Peralta-Zamora, P., Mangrich, A.S., Silvestri, S., 2020. Relationship of the physicochemical properties of novel ZnO/biochar composites to their efficiencies in the degradation of sulfamethoxazole and methyl orange. Sci. Total Environ. 748, 141381. https://doi.org/10.1016/j.scitotenv.2020.141381.

Guan, K., Zhou, P., Zhang, J., Zhu, L., 2020. Synthesis and characterization of ZnO@RSDBC composites and their photo-oxidative degradation of acid Orange 7 in water. J. Mol. Struct. 1203, 127425. https://doi.org/10.1016/j.molstruc.2019.127425.

Guo, J., Yan, C., Luo, Z., Fang, H., Hu, S., Cao, Y., 2019. Synthesis of a novel ternary HA/Fe-Mn oxides-loaded biochar composite and its application in cadmium(II) and arsenic (V) adsorption. J. Environ. Sci. 85, 168–176. https://doi.org/10.1016/j.jes.2019.06.004.

Hassan, M., Liu, Y., Naidu, R., Parikh, S.J., Du, J., Qi, F., et al., 2020. Influences of feedstock sources and pyrolysis temperature on the properties of biochar and functionality as adsorbents: a meta-analysis. Sci. Total Environ. 744, 140714. https://doi.org/10.1016/j.scitotenv.2020.140714.

He, S., Zhong, L., Duan, J., Feng, Y., Yang, B., Yang, L., 2017. Bioremediation of wastewater by Iron oxide-biochar nanocomposites loaded with photosynthetic bacteria. Front. Microbiol. 8, 823. https://doi.org/10.3389/fmicb.2017.00823.

Heidmann, I., Calmano, W., 2008. Removal of Zn(II), Cu(II), Ni(II), Ag(I) and Cr(VI) present in aqueous solutions by aluminium electrocoagulation. J. Hazard. Mater. 152, 934–941. https://doi.org/10.1016/j.jhazmat.2007.07.068.

Heo, J., Yoon, Y., Lee, G., Kim, Y., Han, J., Park, C.M., 2019. Enhanced adsorption of bisphenol A and sulfamethoxazole by a novel magnetic $CuZnFe_2O_4$–biochar composite. Bioresour. Technol. 281, 179–187. https://doi.org/10.1016/j.biortech.2019.02.091.

Hu, H., Sun, L., Wang, T., Lv, C., Gao, Y., Zhang, Y.-F., et al., 2019. Nano-ZnO functionalized biochar as a superhydrophobic biosorbent for selective recovery of low-concentration Re(VII) from strong acidic solutions. Miner. Eng. 142, 105885. https://doi.org/10.1016/j.mineng.2019.105885.

Jung, K.-W., Choi, B.H., Jeong, T.-U., Ahn, K.-H., 2016. Facile synthesis of magnetic biochar/Fe_3O_4 nanocomposites using electro-magnetization technique and its application on the removal of acid orange 7 from aqueous media. Bioresour. Technol. 220, 672–676. https://doi.org/10.1016/j.biortech.2016.09.035.

Jung, K.-W., Lee, S.Y., Lee, Y.J., 2018. Hydrothermal synthesis of hierarchically structured birnessite-type MnO_2/biochar composites for the adsorptive removal of Cu(II) from aqueous media. Bioresour. Technol. 260, 204–212. https://doi.org/10.1016/j.biortech.2018.03.125.

Khataee, A., Kayan, B., Gholami, P., Kalderis, D., Akay, S., Dinpazhoh, L., 2017. Sonocatalytic degradation of reactive yellow 39 using synthesized ZrO_2 nanoparticles on biochar. Ultrasonics - Sonochemistry 39, 540–549. https://doi.org/10.1016/j.ultsonch.2017.05.023.

Kim, J.-S., Sparovek, G., Longo, R.M., De Melo, W.J., Crowley, D., 2007. Bacterial diversity of terra preta and pristine forest soil from the Western Amazon. Soil Biol. Biochem. 39, 684–690. https://doi.org/10.1016/j.soilbio.2006.08.010.

Kim, H., Kim, J., Kim, M., Hyun, S., Moon, D.H., 2018. Sorption of sulfathiazole in the soil treated with giant Miscanthus-derived biochar: effect of biochar pyrolysis temperature, soil pH, and aging period. Environ. Sci. Pollut. Res. 25, 25681–25689. https://doi.org/10.1007/s11356-017-9049-7.

Krasucka, P., Pan, B., Sik Ok, Y., Mohan, D., Sarkar, B., Oleszczuk, P., 2021. Engineered biochar – a sustainable solution for the removal of antibiotics from water. Chem. Eng. J. 405, 126926. https://doi.org/10.1016/j.cej.2020.126926.

Kurniawan, T.A., Chan, G.Y.S., Lo, W.-H., Babel, S., 2006. Physico–chemical treatment techniques for wastewater laden with heavy metals. Chem. Eng. J. 118, 83–98. https://doi.org/10.1016/j.cej.2006.01.015.

Lai, C., Huang, F., Zeng, G., Huang, D., Qin, L., Cheng, M., et al., 2019. Fabrication of novel magnetic $MnFe_2O_4$/bio-char composite and heterogeneous photo-Fenton degradation of tetracycline in near neutral pH. Chemosphere 224, 910–921. https://doi.org/10.1016/j.chemosphere.2019.02.193.

Lehmann, J., Joseph, S., 2009. Biochar for Environmental Management: Science and Technology, London.

Li, R., Wang, J.J., Zhou, B., Zhang, Z., Liu, S., Lei, S., et al., 2017. Simultaneous capture removal of phosphate, ammonium and organic substances by MgO impregnated biochar and its potential use in swine wastewater treatment. J. Clean. Prod. 147, 96–107. https://doi.org/10.1016/j.jclepro.2017.01.069.

Li, C., Zhang, L., Gao, Y., Li, A., 2018a. Facile synthesis of nano ZnO/ZnS modified biochar by directly pyrolyzing of zinc contaminated corn stover for Pb(II), Cu(II) and Cr(VI) removals. Waste Manag. 79, 625–637. https://doi.org/10.1016/j.wasman.2018.08.035.

Li, R., Wang, Z., Zhao, X., Li, X., Xie, X., 2018b. Magnetic biochar-based manganese oxide composite for enhanced fluoroquinolone antibiotic removal from water. Environ. Sci. Pollut. Res. 25, 31136–31148. https://doi.org/10.1007/s11356-018-3064-1.

Li, Ax, Wang, Y., Xiong, X., Liu, H., Wu, N., Liu, R., 2020a. Microstructure and synthesis mechanism of dysprosia-stabilized zirconia nanocrystals via chemical coprecipitation. Ceram. Int. 46, 13331–13341. https://doi.org/10.1016/j.ceramint.2020.02.112.

Li, M., Zhang, Z., Li, Z., Wu, H., 2020b. Removal of nitrogen and phosphorus pollutants from water by $FeCl_3$-impregnated biochar. Ecol. Eng. 149, 105792. https://doi.org/10.1016/j.ecoleng.2020.105792.

Li, X., Xie, Y., Jiang, F., Wang, B., Hu, Q., Tang, Y., et al., 2020c. Enhanced phosphate removal from aqueous solution using resourceable nano-CaO_2/BC composite: behaviors and mechanisms. Sci. Total Environ. 709, 136123. https://doi.org/10.1016/j.scitotenv.2019.136123.

Lian, G., Wang, B., Lee, X., Li, L., Liu, T., Lyu, W., 2019. Enhanced removal of hexavalent chromium by engineered biochar composite fabricated from phosphogypsum and distillers grains. Sci. Total Environ. 697, 134119. https://doi.org/10.1016/j.scitotenv.2019.134119.

Lin, L., Song, Z., Huang, Y., Khan, Z.H., Qiu, W., 2019. Removal and oxidation of arsenic from aqueous solution by biochar impregnated with Fe-Mn oxides. Water Air Soil Pollut. 230, 105. https://doi.org/10.1007/s11270-019-4146-5.

Liu, Y., Li, Y., Huang, J., Zhang, Y., Ruan, Z., Hu, T., et al., 2019. An advanced sol-gel strategy for enhancing interfacial reactivity of iron oxide nanoparticles on rosin biochar substrate to remove Cr(VI). Sci. Total Environ. 690, 438–446. https://doi.org/10.1016/j.scitotenv.2019.07.021.

Liu, J., Jiang, J., Meng, Y., Aihemaiti, A., Xu, Y., Xiang, H., et al., 2020. Preparation, environmental application and prospect of biochar-supported metal nanoparticles: a review. J. Hazard. Mater. 388, 122026. https://doi.org/10.1016/j.jhazmat.2020.122026.

Luo, H., Lin, Q., Zhang, X., Huang, Z., Fu, H., Xiao, R., et al., 2019. Determining the key factors of nonradical pathway in activation of persulfate by metal-biochar nanocomposites for bisphenol A degradation. Chem. Eng. J. 391, 123555. https://doi.org/10.1016/j.cej.2019.123555.

Madikizela, L.M., Ncube, S., Chimuka, L., 2020. Analysis, occurrence and removal of pharmaceuticals in African water resources: a current status. J. Environ. Manag. 253, 109741. https://doi.org/10.1016/j.jenvman.2019.109741.

Mandal, S., Pu, S., He, L., Ma, H., Hou, D., 2020a. Biochar induced modification of graphene oxide & nZVI and its impact on immobilization of toxic copper in soil. Environ. Pollut. 259, 113851. https://doi.org/10.1016/j.envpol.2019.113851.

Mandal, S., Pu, S., Shangguan, L., Liu, S., Ma, H., Adhikari, S., et al., 2020b. Synergistic construction of green tea biochar supported nZVI for immobilization of lead in soil: a mechanistic investigation. Environ. Int. 135, 105374. https://doi.org/10.1016/j.envint.2019.105374.

Mu, B., Wang, A., 2016. Adsorption of dyes onto palygorskite and its composites: a review. J. Environ. Chem. Eng. 4, 1274–1294. https://doi.org/10.1016/j.jece.2016.01.036.

O'Connor, D., Peng, T., Zhang, J., Tsang, D.C.W., Alessi, D.S., Shen, Z., et al., 2018. Biochar application for the remediation of heavy metal polluted land: a review of in situ field trials. Sci. Total Environ. 619–620, 815–826. https://doi.org/10.1016/j.scitotenv.2017.11.132.

Oginni, O., Yakaboylu, G.A., Singh, K., Sabolsky, E.M., Unal-Tosun, G., Jaisi, D., et al., 2020. Phosphorus adsorption behaviors of MgO modified biochars derived from waste woody biomass resources. J. Environ. Chem. Eng. 8, 103723. https://doi.org/10.1016/j.jece.2020.103723.

Ok, Y.S., Bhatnagar, A., Hou, D., Bhaskar, T., Masek, O., 2020. Advances in algal biochar: production, characterization and applications. Bioresour. Technol. 317, 123982. https://doi.org/10.1016/j.biortech.2020.123982.

Ouyang, D., Yan, J., Qian, L., Chen, Y., Han, L., Su, A., et al., 2017. Degradation of 1,4-dioxane by biochar supported nano magnetite particles activating persulfate. Chemosphere 184, 609–617. https://doi.org/10.1016/j.chemosphere.2017.05.156.

Peng, G., Jiang, S., Wang, Y., Zhang, Q., Cao, Y., Sun, Y., et al., 2020. Synthesis of Mn/Al double oxygen biochar from dewatered sludge for enhancing phosphate removal. J. Clean. Prod. 251, 119725. https://doi.org/10.1016/j.jclepro.2019.119725.
Penke, Y.K., Anantharaman, G., Ramkumar, J., Kar, K.K., 2019. Redox synergistic Mn-Al-Fe and Cu-Al-Fe ternary metal oxide nano adsorbents for arsenic remediation with environmentally stable As(0) formation. J. Hazard. Mater. 364, 519–530. https://doi.org/10.1016/j.jhazmat.2018.10.069.
Qian, K., Kumar, A., Zhang, H., Bellmer, D., Huhnke, R., 2015. Recent advances in utilization of biochar. Renew. Sust. Energ. Rev. 42, 1055–1064. https://doi.org/10.1016/j.rser.2014.10.074.
Qian, L., Zhang, W., Yan, J., Han, L., Gao, W., Liu, R., et al., 2016. Effective removal of heavy metal by biochar colloids under different pyrolysis temperatures. Bioresour. Technol. 206, 217–224. https://doi.org/10.1016/j.biortech.2016.01.065.
Qin, Y., Zhu, X., Su, Q., Anumah, A., Gao, B., Lyu, W., et al., 2019. Enhanced removal of ammonium from water by ball-milled biochar. Environ. Geochem. Health https://doi.org/10.1007/s10653-019-00474-5.
Qiu, Y., Xu, X., Xu, Z., Liang, J., Yu, Y., Cao, X., 2020. Contribution of different iron species in the iron-biochar composites to sorption and degradation of two dyes with varying properties. Chem. Eng. J. 389, 124471. https://doi.org/10.1016/j.cej.2020.124471.
Saravanakumar, R., Muthukumaran, K., Selvaraju, N., 2019. Enhanced Pb(II) ions removal by using magnetic NiO/biochar composite. Mater. Res. Express 6, 105504. https://doi.org/10.1088/2053-1591/ab2141.
Shang, J., Pi, J., Zong, M., Wang, Y., Li, W., Liao, Q., 2016. Chromium removal using magnetic biochar derived from herb-residue. J. Taiwan Inst. Chem. Eng. 68, 289–294. https://doi.org/10.1016/j.jtice.2016.09.012.
Shao, B., Dong, D., Wu, Y., Hu, J., Meng, J., Tu, X., et al., 2005. Simultaneous determination of 17 sulfonamide residues in porcine meat, kidney and liver by solid-phase extraction and liquid chromatography–tandem mass spectrometry. Anal. Chim. Acta 546, 174–181. https://doi.org/10.1016/j.aca.2005.05.007.
Shen, Z., Hou, D., Jin, F., Shi, J., Fan, X., Tsang, D.C.W., et al., 2019. Effect of production temperature on lead removal mechanisms by rice straw biochars. Sci. Total Environ. 655, 751–758. https://doi.org/10.1016/j.scitotenv.2018.11.282.
Shen, Q., Wang, Z., Yu, Q., Cheng, Y., Liu, Z., Zhang, T., et al., 2020. Removal of tetracycline from an aqueous solution using manganese dioxide modified biochar derived from Chinese herbal medicine residues. Environ. Res. 183, 109195. https://doi.org/10.1016/j.envres.2020.109195.
Shi, J., Fan, X., Tsang, D.C.W., Wang, F., Shen, Z., Hou, D., et al., 2019. Removal of lead by rice husk biochars produced at different temperatures and implications for their environmental utilizations. Chemosphere 235, 825–831. https://doi.org/10.1016/j.chemosphere.2019.06.237.
Song, Z., Lian, F., Yu, Z., Zhu, L., Xing, B., Qiu, W., 2014. Synthesis and characterization of a novel MnO_x-loaded biochar and its adsorption properties for Cu^{2+} in aqueous solution. Chem. Eng. J. 242, 36–42. https://doi.org/10.1016/j.cej.2013.12.061.
Tan, G., Wu, Y., Liu, Y., Xiao, D., 2018. Removal of Pb(II) ions from aqueous solution by manganese oxide coated rice straw biochar A low-cost and highly effective sorbent. J. Taiwan Inst. Chem. Eng. 84, 85–92. https://doi.org/10.1016/j.jtice.2017.12.031.
Tang, Q., Shi, C., Shi, W., Huang, X., Ye, Y., Jiang, W., et al., 2019. Preferable phosphate removal by nano-La(III) hydroxides modified mesoporous rice husk biochars: role of the host pore structure and point of zero charge. Sci. Total Environ. 662, 511–520. https://doi.org/10.1016/j.scitotenv.2019.01.159.
Wan, S., Wu, J., Zhou, S., Wang, R., Gao, B., He, F., 2018. Enhanced lead and cadmium removal using biochar-supported hydrated manganese oxide (HMO) nanoparticles: behavior and mechanism. Sci. Total Environ. 616–617, 1298–1306. https://doi.org/10.1016/j.scitotenv.2017.10.188.
Wan, X., Li, C., Parikh, S.J., 2020. Simultaneous removal of arsenic, cadmium, and lead from soil by iron-modified magnetic biochar. Environ. Pollut. 261, 114157. https://doi.org/10.1016/j.envpol.2020.114157.
Wang, J., Wang, S., 2019. Preparation, modification and environmental application of biochar: a review. J. Clean. Prod. 227, 1002–1022. https://doi.org/10.1016/j.jclepro.2019.04.282.
Wang, J., Zhuan, R., 2020. Degradation of antibiotics by advanced oxidation processes: an overview. Sci. Total Environ. 701, 135023. https://doi.org/10.1016/j.scitotenv.2019.135023.
Wang, B., Lehmann, J., Hanley, K., Hestrin, R., Enders, A., 2015a. Adsorption and desorption of ammonium by maple wood biochar as a function of oxidation and pH. Chemosphere 138, 120–126. https://doi.org/10.1016/j.chemosphere.2015.05.062.
Wang, M.C., Sheng, G.D., Qiu, Y.P., 2015b. A novel manganese-oxide/biochar composite for efficient removal of lead(II) from aqueous solutions. Int. J. Environ. Sci. Technol. 12, 1719–1726. https://doi.org/10.1007/s13762-014-0538-7.
Wang, B., Lehmann, J., Hanley, K., Hestrin, R., Enders, A., 2016. Ammonium retention by oxidized biochars produced at different pyrolysis temperatures and residence times. RSC Adv. 6, 41907–41913. https://doi.org/10.1039/c6ra06419a.
Wang, B., Gao, B., Fang, J., 2017. Recent advances in engineered biochar productions and applications. Crit. Rev. Environ. Sci. Technol. 47, 2158–2207. https://doi.org/10.1080/10643389.2017.1418580.
Wang B, Gao B, Wan Y, 2018a. Entrapment of ball-milled biochar in Ca-alginate beads for the removal of aqueous Cd(II). Journal of Industrial and Engineering Chemistry 61, 161–168. doi:10.1016/j.jiec.2017.12.013.
Wang, B., Gao, B., Zimmerman, A.R., Zheng, Y., Lyu, H., 2018b. Novel biochar-impregnated calcium alginate beads with improved water holding and nutrient retention properties. J. Environ. Manag. 209, 105–111. https://doi.org/10.1016/j.jenvman.2017.12.041.
Wang, B., Wan, Y., Zheng, Y., Lee, X., Liu, T., Yu, Z., et al., 2018c. Alginate-based composites for environmental applications: a critical review. Crit. Rev. Environ. Sci. Technol. 49, 318–356. https://doi.org/10.1080/10643389.2018.1547621.
Wang, C., Wang, H., Cao, Y., 2018d. Pb(II) sorption by biochar derived from Cinnamomum camphora and its improvement with ultrasound-assisted alkali activation. Colloids Surf. A Physicochem. Eng. Asp. 556, 177–184. https://doi.org/10.1016/j.colsurfa.2018.08.036.
Wang B, Gao B, Wan Y, 2019a. Comparative study of calcium alginate, ball-milled biochar, and their composites on aqueous methylene blue adsorption. Environmental Science and Pollution Research 26, 11535–11541. https://doi.org/10.1007/s11356-018-1497-1.
Wang, C., Tan, H., Liu, H., Wu, B., Xu, F., Xu, H., 2019b. A nanoscale ferroferric oxide coated biochar derived from mushroom waste to rapidly remove Cr(VI) and mechanism study. Bioresource Technology Reports 7, 100253. https://doi.org/10.1016/j.biteb.2019.100253.
Wang, L., Wang, Y., Ma, F., Tankpa, V., Bai, S., Guo, X., et al., 2019c. Mechanisms and reutilization of modified biochar used for removal of heavy metals from wastewater: a review. Sci. Total Environ. 668, 1298–1309. https://doi.org/10.1016/j.scitotenv.2019.03.011.
Wang, S., Zhao, M., Zhou, M., Li, Y.C., Wang, J., Gao, B., et al., 2019d. Biochar-supported nZVI (nZVI/BC) for contaminant removal from soil and water: a critical review. J. Hazard. Mater. 373, 820–834. https://doi.org/10.1016/j.jhazmat.2019.03.080.
Wang, Y., Wang, L., Deng, X., Gao, H., 2019e. A facile pyrolysis synthesis of biochar/ZnO passivator: immobilization behavior and mechanisms for Cu (II) in soil. Environ. Sci. Pollut. Res. 27, 1888–1897. https://doi.org/10.1007/s11356-019-06888-z.
Wang, B., Lian, G., Lee, X., Gao, B., Li, L., Liu, T., et al., 2020a. Phosphogypsum as a novel modifier for distillers grains biochar removal of phosphate from water. Chemosphere 238, 124684. https://doi.org/10.1016/j.chemosphere.2019.124684.
Wang, L., Bolan, N.S., Tsang, D.C.W., Hou, D., 2020b. Green immobilization of toxic metals using alkaline enhanced rice husk biochar: effects of pyrolysis temperature and KOH concentration. Sci. Total Environ. 720, 137584. https://doi.org/10.1016/j.scitotenv.2020.137584.
Wang L, Chen L, Tsang DCW, Guo B, Yang J, Shen Z, et al., 2020c. Biochar as green additives in cement-based composites with carbon dioxide curing. Journal of Cleaner Production 258, 120678. https://doi.org/10.1016/j.jclepro.2020.120678.
Wen E, Yang X, Chen H, Shaheen SM, Sarkar B, Xu S, et al., 2020. Iron-modified biochar and water management regime-induced changes in plant growth, enzyme activities, and phytoavailability of arsenic, cadmium and lead in a paddy soil. Journal of Hazardous Materials 124344. doi:https://doi.org/10.1016/j.jhazmat.2020.124344.
Wu, Y., Gao, M., Chen, W., Lü, Z., Yu, S., Liu, M., et al., 2020a. Efficient removal of anionic dye by constructing thin-film composite membrane with high perm-selectivity and improved anti-dye-deposition property. Desalination 476, 114228. https://doi.org/10.1016/j.desal.2019.114228.
Wu, Z., Chen, X., Yuan, B., Fu, M.-L., 2020b. A facile foaming-polymerization strategy to prepare 3D MnO_2 modified biochar-based porous hydrogels for efficient removal of Cd(II) and Pb(II). Chemosphere 239, 124745. https://doi.org/10.1016/j.chemosphere.2019.124745.
Xiang, Y., Yang, X., Xu, Z., Hu, W., Zhou, Y., Wan, Z., et al., 2020. Fabrication of sustainable manganese ferrite modified biochar from vinasse for enhanced adsorption of fluoroquinolone antibiotics: effects and mechanisms. Sci. Total Environ. 709, 136079. https://doi.org/10.1016/j.scitotenv.2019.136079.
Xiao, R., Wang, J.J., Li, R., Park, J., Meng, Y., Zhou, B., et al., 2018. Enhanced sorption of hexavalent chromium [Cr(VI)] from aqueous solutions by diluted sulfuric acid-assisted MgO-coated biochar composite. Chemosphere 208, 408–416. https://doi.org/10.1016/j.chemosphere.2018.05.175.
Xu, K., Lin, F., Dou, X., Zheng, M., Tan, W., Wang, C., 2018. Recovery of ammonium and phosphate from urine as value-added fertilizer using wood waste biochar loaded with magnesium oxides. J. Clean. Prod. 187, 205–214. https://doi.org/10.1016/j.jclepro.2018.03.206.
Xu, K., Zhang, C., Dou, X., Ma, W., Wang, C., 2019. Optimizing the modification of wood waste biochar via metal oxides to remove and recover phosphate from human urine. Environ. Geochem. Health 41, 1767–1776. https://doi.org/10.1007/s10653-017-9986-6.
Xu, H., Zhang, Y., Li, J., Hao, Q., Li, X., Liu, F., 2020a. Heterogeneous activation of peroxymonosulfate by a biochar-supported Co_3O_4 composite for efficient degradation of chloramphenicols. Environ. Pollut. 257, 113610. https://doi.org/10.1016/j.envpol.2019.113610.
Xu, Z., Xu, X., Zhang, Y., Yu, Y., Cao, X., 2020b. Pyrolysis-temperature depended electron donating and mediating mechanisms of biochar for Cr(VI) reduction. J. Hazard. Mater. 388, 121794. https://doi.org/10.1016/j.jhazmat.2019.121794.
Yang, B., Zhang, M., Wu, M., Zhang, H., Song, Q., Yu, S., 2019. Synthesis of biochar-based Cu_2O nanoparticles and their antibacterial activity against *Escherichia coli*. Inorg. Nano-Met. Chem. 49, 12–16. https://doi.org/10.1080/24701556.2019.1571512.
Yao, Y., Gao, B., Chen, J., Yang, L., 2013a. Engineered biochar reclaiming phosphate from aqueous solutions: mechanisms and potential application as a slow-release fertilizer. Environmental Science & Technology 47, 8700–8708. https://doi.org/10.1021/es4012977.
Yao, Y., Gao, B., Chen, J., Zhang, M., Inyang, M., Li, Y., et al., 2013b. Engineered carbon (biochar) prepared by direct pyrolysis of Mg-accumulated tomato tissues: characterization and phosphate removal potential. Bioresour. Technol. 138, 8–13. https://doi.org/10.1016/j.biortech.2013.03.057.
Yi, Y., Huang, Z., Lu, B., Xian, J., Tsang, E.P., Cheng, W., et al., 2020. Magnetic biochar for environmental remediation: a review. Bioresour. Technol. 298, 122468. https://doi.org/10.1016/j.biortech.2019.122468.
Yin, Z., Xu, S., Liu, S., Xu, S., Li, J., Zhang, Y., 2020. A novel magnetic biochar prepared by K_2FeO_4-promoted oxidative pyrolysis of pomelo peel for adsorption of hexavalent chromium. Bioresour. Technol. 300, 122680. https://doi.org/10.1016/j.biortech.2019.122680.
Yu, Z., Zhou, L., Huang, Y., Song, Z., Qiu, W., 2015. Effects of a manganese oxide-modified biochar composite on adsorption of arsenic in red soil. J. Environ. Manag. 163, 155–162. https://doi.org/10.1016/j.jenvman.2015.08.020.

Yu, Z., Qiu, W., Wang, F., Lei, M., Wang, D., Song, Z., 2017. Effects of manganese oxide-modified biochar composites on arsenic speciation and accumulation in an indica rice (*Oryza sativa L.*) cultivar. Chemosphere 168, 341–349. https://doi.org/10.1016/j.chemosphere.2016.10.069.

Yu, J., Jiang, C., Guan, Q., Ning, P., Gu, J., Chen, Q., et al., 2018. Enhanced removal of Cr(VI) from aqueous solution by supported ZnO nanoparticles on biochar derived from waste water hyacinth. Chemosphere 195, 632–640. https://doi.org/10.1016/j.chemosphere.2017.12.128.

Yuan, Q., He, Y., Mao, B., Zuo, P., Wu, W., Huang, Y., et al., 2020. Nano-metal oxides naturally attenuate antibiotic resistance in wastewater: killing antibiotic resistant bacteria by dissolution and decreasing antibiotic tolerance by attachment. NanoImpact 18, 100225. https://doi.org/10.1016/j.impact.2020.100225.

Zhai, S., Li, M., Wang, D., Zhang, L., Yang, Y., Fu, S., 2019. In situ loading metal oxide particles on bio-chars: reusable materials for efficient removal of methylene blue from wastewater. J. Clean. Prod. 220, 460–474. https://doi.org/10.1016/j.jclepro.2019.02.152.

Zhang, M., Gao, B., Yao, Y., Xue, Y., Inyang, M., 2012. Synthesis of porous MgO-biochar nanocomposites for removal of phosphate and nitrate from aqueous solutions. Chem. Eng. J. 210, 26–32. https://doi.org/10.1016/j.cej.2012.08.052.

Zhang, J., Hou, D., Shen, Z., Jin, F., O'Connor, D., Pan, S., et al., 2020a. Effects of excessive impregnation, magnesium content, and pyrolysis temperature on MgO-coated watermelon rind biochar and its lead removal capacity. Environ. Res. 183, 109152. https://doi.org/10.1016/j.envres.2020.109152.

Zhang JY, Zhou H, Gu JF, Huang F, Yang WJ, Wang SL, et al., 2020b. Effects of nano-Fe_3O_4-modified biochar on iron plaque formation and Cd accumulation in rice (*Oryza sativa L.*). Environmental Pollution 260, 113970. doi:https://doi.org/10.1016/j.envpol.2020.113970.

Zhang, P., O'Connor, D., Wang, Y., Jiang, L., Xia, T., Wang, L., et al., 2020c. A green biochar/iron oxide composite for methylene blue removal. J. Hazard. Mater. 384, 121286. https://doi.org/10.1016/j.jhazmat.2019.121286.

Zhang, X., Sun, P., Wei, K., Huang, X., Zhang, X., 2020d. Enhanced H_2O_2 activation and sulfamethoxazole degradation by Fe-impregnated biochar. Chem. Eng. J. 385, 123921. https://doi.org/10.1016/j.cej.2019.123921.

Zhao, B., O'Connor, D., Zhang, J., Peng, T., Shen, Z., Tsang, D.C.W., et al., 2018. Effect of pyrolysis temperature, heating rate, and residence time on rapeseed stem derived biochar. J. Clean. Prod. 174, 977–987. https://doi.org/10.1016/j.jclepro.2017.11.013.

Zhao, B., O'Connor, D., Shen, Z., Tsang, D.C.W., Rinklebe, J., Hou, D., 2020. Sulfur-modified biochar as a soil amendment to stabilize mercury pollution: an accelerated simulation of long-term aging effects. Environ. Pollut. 264, 114687. https://doi.org/10.1016/j.envpol.2020.114687.

Zheng, Y., Wan, Y., Chen, J., Chen, H., Gao, B., 2020. MgO modified biochar produced through ball milling: a dual-functional adsorbent for removal of different contaminants. Chemosphere 243, 125344. https://doi.org/10.1016/j.chemosphere.2019.125344.

Zhou, J.L., Zhang, Z.L., Banks, E., Grover, D., Jiang, J.Q., 2009. Pharmaceutical residues in wastewater treatment works effluents and their impact on receiving river water. J. Hazard. Mater. 166, 655–661. https://doi.org/10.1016/j.jhazmat.2008.11.070.

Zhou, L., Huang, Y., Qiu, W., Sun, Z., Liu, Z., Song, Z., 2017. Adsorption properties of nano-MnO_2-biochar composites for copper in aqueous solution. Molecules 22, 173. https://doi.org/10.3390/molecules22010173.

Zhou, Q., Liao, B., Lin, L., Qiu, W., Song, Z., 2018. Adsorption of Cu(II) and Cd(II) from aqueous solutions by ferromanganese binary oxide-biochar composites. Sci. Total Environ. 615, 115–122. https://doi.org/10.1016/j.scitotenv.2017.09.220.

Zhou, Y., Lu, J., Zhou, Y., Liu, Y., 2019. Recent advances for dyes removal using novel adsorbents: a review. Environ. Pollut. 252, 352–365. https://doi.org/10.1016/j.envpol.2019.05.072.

Zhu, Z., Huang, C.P., Zhu, Y., Wei, W., Qin, H., 2018. A hierarchical porous adsorbent of nano-α-Fe_2O_3/Fe_3O_4 on bamboo biochar (HPA-Fe/C-B) for the removal of phosphate from water. J. Water Process Eng. 25, 96–104. https://doi.org/10.1016/j.jwpe.2018.05.010.

Zhu, D., Chen, Y., Yang, H., Wang, S., Wang, X., Zhang, S., et al., 2020a. Synthesis and characterization of magnesium oxide nanoparticle-containing biochar composites for efficient phosphorus removal from aqueous solution. Chemosphere 247, 125847. https://doi.org/10.1016/j.chemosphere.2020.125847.

Zhu, Y., Dai, W., Deng, K., Pan, T., Guan, Z., 2020b. Efficient removal of Cr(VI) from aqueous solution by Fe-Mn oxide-modified biochar. Water Air Soil Pollut. 231, 61. https://doi.org/10.1007/s11270-020-4432-2.

Zhu, Y., Fan, W., Zhang, K., Xiang, H., Wang, X., 2020c. Nano-manganese oxides-modified biochar for efficient chelated copper citrate removal from water by oxidation-assisted adsorption process. Sci. Total Environ. 709, 136154. https://doi.org/10.1016/j.scitotenv.2019.136154.